7-2013

Coupling Fast Water Exchange to Slow Molecular Tumbling in Gd3+ Chelates: Why Faster Is Not Always Better

Stefano Avedano
Università del Piemonte Orientale

Mauro Botta
Università del Piemonte Orientale

Julian Saunders Haigh
Portland State University, julianshaigh@gmail.com

Dario L. Lango
Università di Torino

Mark Woods
Portland State University, mark.woods@pdx.edu

Citation Details

Published as: Avedano, S., Botta, M., Haigh, J., Longo, D., and Woods, M. (2013). Coupling fast water exchange to slow molecular tumbling in Gd3+ chelates: why faster is not always better. Inorg. Chem., 2013, 52, 8436-8450.

Published in final edited form as:
Inorg Chem. 2013 August 5; 52(15): 8436–8450. doi:10.1021/ic400308a.

Coupling fast water exchange to slow molecular tumbling in Gd^{3+} chelates: why faster is not always better

Stefano Avedano[†], **Mauro Botta**[†,*], **Julian S. Haigh**[§], **Dario Longo**[‰], and **Mark Woods**[§,‡,*]

[†] Dipartimento di Scienze e Innovazione Tecnologica, Università del Piemonte Orientale "Amedeo Avogadro", Viale T. Michel 11, I-15121 Alessandria, Italy.

[§] Department of Chemistry, Portland State University, 1719 SW 10th Ave, Portland, OR 97201, USA.

[‰] Dipartimento di Biotecnologie Molecolari e Scienze della Salute and Molecular Imaging Center, Università di Torino, Via Nizza 52, I-10126 Torino, Italy.

[‡] Advanced Imaging Research Center, Oregon Health & Science University, 3181 S.W. Sam Jackson Park Road, Portland, OR 97239, USA.

Abstract

The influence of dynamics on solution state structure is a widely overlooked consideration in chemistry. Variations in Gd^{3+} chelate hydration with changing coordination geometry and dissociative water exchange kinetics substantially impact the effectiveness (or relaxivity) of mono-hydrated Gd^{3+} chelates as T_1-shortening contrast agents for MRI. Theory shows that relaxivity is highly dependent upon the Gd^{3+}-water proton distance (r_{GdH}) and yet this distance is almost never considered as a variable in assessing the relaxivity of a Gd^{3+} chelate as a potential contrast agent. The consequence of this omission can be seen when considering the relaxivity of isomeric Gd^{3+} chelates that exhibit different dissociative water exchange kinetics. The results described herein show that the relaxivity of a chelate with 'optimal' dissociative water exchange kinetics is actually lower than that of an isomeric chelate with 'sub-optimal' dissociative water exchange. When the rate of molecular tumbling of these chelates is slowed, an approach that has long been understood to increase relaxivity, the observed difference in relaxivity is increased with the more rapidly exchanging ('optimal') chelate exhibiting lower relaxivity than the 'sub-optimally' exchanging isomer. The difference between the chelates arises from a non-field dependent parameter: either the hydration number (q) or r_{GdH}. For solution state Gd^{3+} chelates, changes in the values of q and r_{GdH} are indistinguishable. These parametric expressions simply describe the hydration *state* of the chelate – *i.e.* the number and position of closely associating water molecules. The hydration state (q/r_{GdH}^6) of a chelate is intrinsically linked to its dissociative water exchange rate k_{ex} and the interrelation of these parameters must be considered when examining the relaxivity of Gd^{3+} chelates. The data presented herein indicates that the changes in the hydration parameter (q/r_{GdH}^6) associated with changing dissociative water exchange kinetics has a profound effect on relaxivity and suggest that achieving the highest relaxivities in monohydrated Gd^{3+} chelates is more complicated than simply "optimizing" dissociative water exchange kinetics.

[*]**Corresponding Author** MB: mauro.botta@unipmn.it; Tel: +39-0131-360253: MW: mark.woods@pdx.edu or woodsmar@ohsu.edu; Tel: + 1-503-725-8238 or 1-503-418-5530.

Supporting Information. Details of the cmc determination, emission spectra of *S-RRR*-Eu**4** and *S-SSS*-Eu**4**, full NMRD profiles of all slowly rotating systems, displacement and relaxometric titrations and to determine HSA binding. This material is available free of charge via the Internet at http://pubs.acs.org.

The authors declare no competing financial interests.

Keywords

Coordination isomers; Dissociative water exchange; Gadolinium chelates; HSA binding; MRI contrast agents

Introduction

Chelates of Gd^{3+} are now routinely administered as contrast agents for MRI. After intravenous injection these chelates extravasate through the pores at the endothelial junctions of the vasculature into interstitial space. Time dependent modulation of the dipolar interactions between the seven unpaired electrons of Gd^{3+} and proximate water protons leads to a shortening of the water proton longitudinal relaxation time constant (T_1). In T_1-weighted MR images this results in enhanced signal intensity in those regions to which the agent is distributed. For agents that are currently in clinical use, distribution is a function of a number of vasculature characteristics, such as blood flow and pore size; and the size of the agent. The limited criteria by which these agents discriminate between tissue types limits the diagnostic information that can be obtained by administering these contrast agents. These limitations have provoked the idea of a new class of contrast agent: so-called “targeted agents” would possess a structural component that is designed to bind to a biomarker associated with a disease of interest.[1] Binding of the agent will increase the localization of the agent in regions where that biomarker is more abundant, thereby increasing MR signal intensity of regions associated with the disease. Binding has one further effect: it will slow the agent's rate of molecular tumbling, characterized by the correlation time τ_R.

The theory of paramagnetic relaxation given by the Solomon-Bloembergen-Morgan (SBM) equations (equations 1-3) describes the relaxation of water protons that occurs through exchange of water molecules coordinated directly to the paramagnetic metal center.[2-6] These equations tell us that reducing the rate of molecular tumbling (making τ_R longer) will afford a more effective contrast agent.[7-9] This is critical because the Gd^{3+} chelates that are currently used clinically have high detection limits; a typical dose (0.1 $mmolkg^{-1}$) equates to about 4.5 g of agent in a single bolus for a 70 kg human. Clearly, if biomarkers of disease, which are present only in very low abundance, are to be detected by MRI then it is absolutely critical that the detection limit of any “targeted agent” be much lower than those of agents currently employed. To this end the SBM equations have been used to guide research into improving the function of MRI contrast agents. These equations reveal several parameters that may be manipulated by the chemist to control the effectiveness of an agent – defined as the longitudinal relaxivity, r_1. From the SBM equations τ_R is found to limit the relaxivity of low molecular weight clinical agents. τ_R is readily made longer either by increasing the size of the agent, or by coupling its molecular motion to that of a large (or stationary) structure such as a protein or cell. However, it is commonly found that when τ_R is made longer the relaxivity of a Gd^{3+} chelate is subsequently limited by the kinetics of inner. sphere water exchange.[10] If τ_M, the residence lifetime of a water molecule on Gd^{3+}, is too long then the coordination site on $Gd^{3+}$is needlessly occupied by a ‘relaxed’ water molecule preventing relaxation of other water molecules, slowing the catalysis of bulk relaxation by the relaxation agent. This is the situation that prevails in all clinically approved Gd^{3+} chelates; if the limiting effect of τ_R is lifted then slow water exchange kinetics become limiting and the highest relaxivities are not realized.[10] This realization has prompted considerable research effort into the development of more rapidly exchanging Gd^{3+} chelates that would, in principle, afford the highest relaxivities if the limiting effect of τ_R were lifted.

$$r_1^{is} = \frac{q}{55.5}\left(\frac{1}{T_{1M}+\tau_M}\right) \quad (1)$$

$$\frac{1}{T_{1M}} = \frac{2}{15}\left(\frac{\mu_0}{4\pi}\right)^2 \gamma_H^2 \gamma_S^2 \hbar^2 S\,(S+1)\,\frac{1}{r_{GdH}^6}\left[\frac{7\tau_{c2}}{1+(\omega_S\tau_{c2})^2}+\frac{3\tau_{c1}}{1+(\omega_H\tau_{c1})^2}\right] \quad (2)$$

$$\frac{1}{\tau_{Ci}} = \frac{1}{\tau_M}+\frac{1}{\tau_R}+\frac{1}{T_{ie}} \quad i=1,2 \quad (3)$$

Several other parameters expressed in the SBM equations are also potentially under the control of the chemist. Relaxivity scales proportionally with the number of water molecules coordinated directly to the Gd^{3+} ion, *q*, so increasing the number of water molecules directly coordinated to Gd^{3+} will afford higher relaxivities. However, increasing the number of vacant coordination sites on Gd^{3+} is also found to reduce the stability of the chelate. Unchelated, the Gd^{3+} ion is quite toxic to mammals (LD_{50} ~ 0.35 $mmolkg^{-1}$, *i.v.* in mice)[11] and must therefore be administered in the form of a kinetically and thermodynamically robust chelate.[10,12] In all clinically approved agents the Gd^{3+} ion is chelated by an octadentate polyaminocarboxylate ligand (DTPA or a derivative, or DOTA or a derivative) and this leaves one coordination site available for occupation by water. Opening additional coordination sites to water, and therefore decreasing the sites coordinated by the chelating ligand, is generally found to cause the stability constant of a chelate to drop by as much as 3 orders of magnitude;[13] suggesting that in practice, with perhaps a few exceptions,[14-16] only $q = 1$ chelates are suitable for *in vivo* use.

The recent observation of nephrogenic systemic fibrosis (NSF) in some renally compromised patients after administration of DPTA-based contrast agents further highlights the importance of chelate stability as a consideration in contrast agent development.[17,18] Even though Gd^{3+} chelates derived from DTPA are $q = 1$ chelates, it is now generally accepted that they are not sufficiently robust to survive prolonged *in vivo* residence completely intact and are only safe if the entire dose is excreted rapidly.[12,19-21] Targeted imaging applications also envisage prolonged *in vivo* residence lifetimes and as such Gd^{3+} chelates derived from DTPA should not be considered suited for the purpose. The Gd^{3+} chelates of DOTA and its derivatives are more thermodynamically stable and more kinetically robust than their DTPA counterparts.[22] They are more suitable for applications that require prolonged *in vivo* lifetimes, and controversy surrounds the isolated cases in which GdDOTA has been associated cases of NSF.[23] In general, DOTA derivatives are considered sufficiently stable for prolonged *in vivo* residence lifetimes, and therefore for targeted applications. A further advantage of DOTA-derived chelates is the superior electron spin relaxation characteristics (T_{1e} and T_{2e}) of these chelates. Electron spin relaxation is sometimes cited as another modifiable parameter that regulates relaxivity. However, even though considerable effort is being made to better understand this parameter,[24-27] at present its relationship with coordination chemistry is vague at best and at present the chemist is really faced with accepting what a given chelate provides. However, in general DOTA derivatives are on the whole found to exhibit somewhat more favorable electron spin relaxation characteristics than their DTPA-based counterparts.[28]

Finally, one further parameter that also relates to hydration of the chelate can potentially have a profound effect upon relaxivity. The distance from the metal to the inner sphere water protons, r_{GdH}, is most widely viewed as a fixed value. In spite of this, the value used

in the calculations and fitting of relaxation data of Gd^{3+} chelates varies quite a bit; with values anywhere from 2.9 to 3.1 Å commonly used.[29] Given that relaxivity scales to the negative sixth power of r_{GdH}, even small changes in this value would be expected to have profound effects on relaxivity. Parker and co-workers have demonstrated that faster dissociative water exchange kinetics are associated with weaker (*i.e.* longer) Gd^{3+}-OH_2 bonds.[30,31] Our own results suggest that differences in r_{GdH} associated with differing dissociative water exchange rates may not be confined solely to consideration of "*bond*" distances but that the differences in r_{GdH} may be even greater in solution.[32-34] These differences in r_{GdH} are comparatively small – certainly less than the range of values commonly employed in the published data analyses. Such small variations in r_{GdH} are very difficult to quantify – they are less than the reported uncertainty in ENDOR measurements for instance,[35] and yet they could be large enough that they significantly impact relaxivity.

Several research groups around the world, including ourselves, have developed $q = 1$ Gd^{3+} chelates that possess very fast dissociative water exchange kinetics.[36-41] However, our chosen approach is unique in that in addition to a chelate with very fast dissociative water exchange kinetics the same methods can be applied to generate an *isomeric* chelate with slower dissociative water exchange kinetics.[34,42] This allows us, for the first time, to compare the effects of accelerating inner-sphere dissociative water exchange on relaxivity. To achieve this aim in slowly tumbling chelates, we have prepared prototypical targeted contrast agents that employ a simple hydrophobic group that will cause the agent to bind to various slowly tumbling systems, such as human serum albumin (HSA). The advantages of this approach are that it is easy to achieve and binding to HSA is comparatively well understood; furthermore it also allows our results to be compared to those obtained for related systems that also bind HSA.

Results and Discussion

Gd^{3+} chelates of DOTA-type ligands can exist in two coordination geometries: a square antiprism (SAP) and a twisted square antiprism (TSAP). It has long been appreciated that the water exchange kinetics of the TSAP isomer are considerably faster than those of the SAP isomer.[33,43] To attain the highest relaxivities a TSAP isomer should therefore be the preferred coordination geometry. In solution these two coordination isomers can interconvert and a mixture of both is usually observed – for GdDOTA itself the SAP isomer is found to be the predominant structure (~85%).[44] However, by appropriately substituting the ligand framework the conformational changes by which the two isomers exchange can be 'frozen out', producing a chelate that is 'locked' into a single coordination isomer.[45,46] Careful consideration of the stereochemistry enables one coordination isomer to be selected over the other.[42] The two chelates *S-RRR*-Ln**1** and *S-SSS*-Ln**1** are locked into the SAP and TSAP coordination geometries, respectively (Figure 1). Previous studies have demonstrated that the water exchange kinetics of *S-SSS*-Gd**1** ($\tau_M^{298} \approx 6$ ns) are more or less optimal for attaining the highest relaxivities at current imaging fields (1.5 T).[34] In contrast the water exchange kinetics of *S-RRR*-Gd**1** are considerably slower; $\tau_M^{298} \approx 70$ ns and yet close to the optimal value (~ 20 – 40 ns) predicted for lower magnetic field strengths (0.5 T).[34]

Prototypical 'targeted' contrast agents derived from these conformationally rigid isomeric chelates would allow the effect of varying dissociative water exchange kinetics to be probed in the context of a targeted imaging approach. The two chelates were modified to incorporate a hydrophobic biphenyl group (Gd**4**) that could then be used to slow the rate of molecular tumbling of each chelate through a binding interaction with either poly-β-cyclodextrin (poly-β-CD) or human serum albumin (HSA).

Synthesis

The preparation of the isomeric chelates *S-RRR*-**4** and *S-SSS*-**4** is shown in Scheme 1. The preparation of *S-RRR*-**1** and *S-SSS*-**1** has been reported previously[34] and functionalization of these ligands, by conversion to the corresponding isothiocyanate, is facile.[48] Catalytic hydrogenation using H_2 over 10% palladium on carbon afforded the corresponding primary amines, **2**, in near quantitative conversions. The primary amines **2** were then converted into the isothiocyanates **3** by reaction with thiophosgene. Biphasic reaction conditions were employed with the thiophosgene dissolved in chloroform and the amine **2** dissolved in water at pH 2. The pH of the reaction is crucial to its success since the stability of isothiocyanates decreases as pH rises. Isothiocyanates react readily with primary amines under mildly basic conditions. Accordingly, the isothiocyanates **4** were dissolved in water, the pH raised to 8 with sodium hydroxide and 4-phenylbenzylamine added with dioxane as a co-solvent to facilitate dissolution. After stirring for 24 hours a solution of the appropriate lanthanide chloride in water was added and the reaction stirred at room temperature for a further 48 hours. At periodic intervals the pH of the reaction was monitored and maintained above 6 by addition of sodium hydroxide. The Ln^{3+} chelates of the two biphenyl conjugates *S-RRR*-**4** and *S-SSS*-**4** were isolated and purified by preparative HPLC. Each chelate was isolated as the more favoured 'corner' isomer[47,49] affording the structures shown in Figure 1. The chelates obtained thusly are isolated as the conjugate acid and are poorly soluble in aqueous solution; however, neutralization, by stoichiometric addition of NaOH, affords the chelates as their sodium salts, in which form the chelates are freely soluble in water.

Relaxometric Studies of Biphenyl Conjugates in Solution

The relaxivity of a discrete Gd^{3+} chelate in solution can be determined by measuring the proton relaxation rate constant, R_1 ($= 1/T_1$) over a range of Gd^{3+} concentrations. Because R_1 and $[Gd^{3+}]$ are linearly related in this case, regression analysis of these data affords the relaxivity, r_1, of the chelate from the slope of the line. This standard method of relaxivity determination was applied to the chelates *S-RRR*-Gd**4** and *S-SSS*-Gd**4**. Unexpectedly however, neither chelate exhibited a linear dependence of R_1 on $[Gd^{3+}]$ (Figure 2). In the concentration range 5 to 1 mM linear relationships were observed affording unusually high relaxivity values for each chelate (Table 1 and supplementary information). An abrupt change in the slope of the line is then observed followed by a second linear region over the concentration range 300 to 10 μM. In this region the slope of the line afforded relaxivity values much closer to those normally expected for low molecular weight chelates at 20 MHz and 25 °C (Table 1). This behaviour is very similar to that observed for other Gd^{3+} chelate incorporating a long hydrocarbon groups, such as C17-AAZTA[50] or a GdDOTA-calix[4]arene derivative.[51] As in that case the change in relaxivity can be attributed to the formation of micelles, in which the rotation of Gd^{3+} is slowed, at higher concentrations. Gd^{3+} chelates with large aromatic substituents, such as calix[4]arenes, have previously been shown to form micelles.[51] The critical micelle concentrations (cmc) of the Gd**4** chelates are somewhat below 0.5 mM, in closer agreement with the value determined for C17-AAZTA than calix[4]arene substituted DOTA derivatives (Table 1).[50,51] The relaxivity values of both isomers of Gd**4**, both above and below the cmc, are somewhat higher than found for either the calix[4]arene[49] derivatives or C17-AAZTA.[50] In the former case this is most likely a reflection of the slow exchange kinetics exhibited in this system.[51] The latter case is noteworthy because C17-AAZTA is a $q = 2$ chelate and would therefore be expected to have a somewhat higher relaxivity than either Gd**4** isomer: both $q = 1$ chelates. Given that the water exchange kinetics of C17-AAZTA and *S-RRR*-Gd**4** are comparable this suggests that the primary difference between the chelates must arise from more effective slowing of rotation with the biphenyl substituent relative to that afforded by the hydrocarbon chain, perhaps through continued, weak intermolecular interactions. Strictly analogous behaviour

has also been reported and discussed in the cases of functionalized Gd^{3+} DTPA,[52] DOTA,[53] and EGTA[54] chelates.

The formation of micelles can unambiguously be demonstrated by recording the nuclear magnetic relaxation dispersion (NMRD) profiles of each chelate at concentrations above and below the cmc. The NMRD profiles at low concentrations (0.2 mM) of *S-RRR*-Gd**4** and *S-SSS*-Gd**4** are characteristic of small molecule Gd^{3+} chelates in which relaxivity is limited by τ_R (Figure 3);[10] the relaxivity is higher at very low fields, there is a dispersion around 1 MHz followed by a more gradual decrease in relaxivity at higher fields. However, the profiles have two points of interest. Firstly, the relaxivity of the agents is quite high for discrete chelates, and this can be attributed to either the increase in hydrodynamic volume associated with the inclusion of a bulky biphenyl substituent in the structure, or weak intermolecular associations – reducing the rate of molecular tumbling (longer τ_R). Secondly, and perhaps more significantly, the two curves are *almost* identical across the entire frequency range of the profile, but offset from one another by about 1.5 $mM^{-1}s^{-1}$. This same observation can be made retrospectively for the previously reported NMRD profiles of *S-RRR*-Gd**1** and *S-SSS*-Gd**1**.[34] The fact that these profiles are *almost* superimposable but offset in this way, tells us that the primary difference between the two chelates cannot arise from a parameter whose effect on relaxivity is modulated by changes in B_0 such as τ_M, τ_R, T_{1e} or T_{2e}. There is a very slight additional difference in the dispersions (0.5 to 5 MHz) of the two profiles that suggests a *small* difference in one of these field-dependent parameters. The primary difference between the two chelates must be a parameter with which relaxivity scales directly: in other words either q or r_{GdH}.

Hydration in Ln^{3+} chelates has been something a contentious matter for over a decade now. The disagreements have largely arisen from differing opinions of how to describe differences in hydration between chelates, the debate may appear largely one of semantics but it arises because of the difficulty the scientist faces in describing hydration. Both q and r_{GdH} are parametric descriptors of hydration and the problem is how to define each for a chelate in aqueous solution, and therefore in exchange. It has been possible to account for some of the observed coordination chemistry of the later lanthanides ($Ho^{3+} \rightarrow Lu^{3+}$) by invoking a TSAP coordination isomer that is entirely dehydrated ($q = 0$) in solution.[44,55-57] However, there is no published evidence for the existence of a discrete, dehydrated TSAP isomer of DOTA-type chelates of lanthanides from the middle of the series (Eu^{3+} and Gd^{3+}). In systems where changes in hydration leads to changes in the coordination geometry the non-degenerate $^5D_0 \leftrightarrow {}^7F_0$ transition of the Eu^{3+} ion can be used probe hydration equilibria.[58] The Eu^{3+} coordination geometry in DOTA-type chelates changes only subtly with changing hydration[56] and the high resolution emission spectra (supplementary information, S1) of both *S-RRR*-Eu**4** and *S-SSS*-Eu**4** each exhibit a single line for this transition at about 578 nm. There are three possible explaations for this observation: each chelate has a single hydration species (even though the *S-SSS*-Eu**1** is $q = 0.74$ as determined by Horrocks' method);[31] any change in hydration does not afford sufficient change in the energy of this transition to resolve the different hydration species; or the spectrum affords a time-average of all hydration species in solution.[59] As discussed previously there exists no good method for accurately determining r_{GdH} *in solution*. Although Caravan and co-workers have proposed ENDOR as a means of probing this parameter,[35] it is important to note that those experiments were performed at very low temperatures on static chelates in frozen glasses, a condition that does not in any way resemble the situation of a chelate undergoing exchange in solution. Herein lies the quandary; the hydration states of *S-RRR*-Eu**1** and *S-SSS*-Eu**1** are very different when determined by Horrocks' method – $q = 0.97$ and $q = 0.74$, respectively – how should this difference be interpreted? Insight can be gained from two very different pioneering studies. The work of Parker and co-workers[31] has unambiguously shown that Horrocks' method does not provide simply the hydration number, in fact it

provides *both* the hydration number and the position of those water molecules in a single parameter: *i.e.* Horrocks' hydration *state* describes both q and r_{EuH} in one parameter. Significantly, the hydration *state* also accounts for molecules in the second coordination sphere as well. In his pioneering relaxometric studies on paramagnetic metal ions Bertini, encountered the same problem, and recognizing what Parker would later demonstrate, he used a single parameter to describe the hydration state of the metal ion: q/r_{MH}^6.[60,61] The hydration states of the two Eu**1** chelates determined by Horrocks' method, unambiguously demonstrate a difference in the hydration states of the two chelates.[34] This difference can be represented either as a difference in q, a difference in r_{GdH}, or more properly as a difference in q/r^6. For the purposes of the data analyses performed herein we have employed values of $q/r_{GdH}^6 = 1372\ nm^{-6}$ and $1127\ nm^{-6}$ for *S-RRR*-Gd**4** and *S-SSS*-Gd**4**, respectively. For reasons of simplicity and familiarity these values can be considered to represent two $q = 1$ chelates in which r_{GdH} increases by 0.1 Å or 3.3% (from 3.0 Å to 3.1 Å) on passing from *S-RRR*-Gd**4** to *S-SSS*-Gd**4**. Throughout this article we will employ this description of hydration; however, the reader must recognize two important points: 1) although we will describe q as fixed with only r_{GdH} in variance, in truth either or both hydration parameters may be different between the two chelates; 2) the values of q/r_{GdH}^6 for each chelate are not known, the values, and the difference between them, that are employed herein are more illustrative than precise representations of the hydration in these chelates. However, given the previously noted differences of r_{LnH} (2.8 % in the crystal, 4.5 % in solution)[32-34] between SAP and TSAP isomers the difference seems reasonable and the values of r_{GdH} lie within the range of commonly used values for this type of analysis. Any errors in the values employed will be reflected in deviations in the values of τ_R from the real values. Muller and co-workers have shown that when fitting NMRD profiles variance in the value of r_{GdH}, usually fixed, causes a variance in the obtained value of τ_R.[29] Thus, unless τ_R is independently determined and fixed during fitting, there is some flexibility to the value of r_{GdH} employed provided that the effect on the value of τ_R is appreciated. This flexibility may explain why it has not previously been found necessary to consider the effect of variation in hydration (q/r_{GdH}^6) between chelates when undertaking these fittings.

Taking this approach to hydration both NMRD profiles fit well to theory. In all NMRD fittings herein the water exchange parameter τ_M has been taken from studies on the corresponding isomer of Gd**1**, it is not possible to measure the water exchange kinetics of Gd**4** chelates directly by ^{17}O NMR methods due to solubility constraints. The assumption was made that the peripheral incorporation of a biphenyl group has no significant effect upon the water exchange kinetics of the chelate. The τ_M value for *S-RRR*-Gd**4** was fixed at the value determined for the corresponding isomer of Gd**1**.[34] A variation of this τ_M value by ± 30 ns resulted in a relaxivity change of less than $0.3\ mM^{-1}s^{-1}$ at all fields. In the case of *S-SSS*-Gd**4** fitting was found to be largely insensitive to small changes in τ_M over a range 5 – 10 ns and data were fitted using a τ_M value, 8 ns, that best fits the data. The values of τ_R obtained from fitting the low concentration NMRD profiles of both chelates are somewhat longer than expected for relatively small chelates (Table 2). This may reflect an underestimation of r_{GdH} on our part. Alternatively, these longer than expected values could reflect an increased level of intermolecular π-π interaction (without forming micelles) that will tend to slow rotation and increase relaxivity as discussed earlier. Effects of this type have been observed by Merbach and Helm for other chelates including aromatic groups.[62,63] The similarity in the values of τ_R is expected since the two chelates are isomeric. The parameters Δ^2 and τ_V are reflective of the zero-field splitting and its transient modulation, respectively, which govern the electron spin relaxation time constants of the chelate. In both isomers of Gd**4** the value of τ_V is somewhat different (larger) than is usually obtained in this type of exercise for these types of chelate. Crucially both isomers have very similar electron spin relaxation characteristics, a feature that has been previously established through EPR analysis of analogous chelates to the two isomers of the Gd**1**.[26] Given that the relationship

between electron spin relaxation and coordination chemistry is poorly understood it is difficult to point to a direct physical reason as to why τ_V is longer than might be expected. However, it is worth noting that a marked lengthening of this parameter is very often observed in macromolecular systems.[10,64] That the difference between the two NMRD profiles arises primarily from difference in hydration state between the two chelates is shown by simulating an NMRD profile using the same parameters obtained from the fitting of the profile of *S-RRR*-Gd**4** but extending r_{GdH} from 3.0 to 3.1 Å. This affords a curve that almost exactly fits the experimental data obtained for *S-SSS*-Gd**4** (supplementary information Figure S2), indicating that almost the entire difference between the two profiles is accounted for in the change in r_{GdH}. Furthermore, constraining the hydration states of the two chelates to the same value during fitting affords unrealistic values for other fitting parameters (supplementary Figure S8 and Tables S1 and S2).

The NMRD profiles of the two isomers of Gd**4** recorded at a 3.98 mM, above the cmc, (Figure 4) are characteristic of more slowly tumbling chelates: a classical high field 'hump' is observed in each case indicating the formation of a slowly rotating species, micelles, at higher concentrations. It should be noted that NMRD profiles for slowly rotating systems are shown and fitted herein only in the high field region because of the known limitations of SBM theory in the slowly rotating regime that render it unable to completely account for the behaviour of more slowly rotating chelates at very low magnetic field strengths.[65] These profiles are notable because the high field relaxivity enhancement arising when molecular tumbling is slow (longer τ_R) is greater for *S-RRR*-Gd**4,** the isomer (SAP) with the more slowly exchanging water molecule. This is in direct contrast to the general expectation that more rapid water exchange kinetics (up to an optimal value of about 6 ns at 1.5 T)[7,34] will afford higher relaxivities. Fitting these profiles to SBM theory, incorporating the Lipari-Szabo model,[66,67] affords valuable information about the tumbling dynamics of each chelate in the micelle. The advantage of the Lipari-Szabo model is that it separates the local and global tumbling motions of the chelate, allowing the effect of local molecular motion on relaxivity to be considered. Fitting was undertaken with the aforementioned difference of 0.1 Å in the values of r_{GdH} used for the two isomeric chelates. The fits afforded comparable values of τ_g and τ_l; the global and local molecular tumbling correlation times, respectively. These results indicate that the micelles formed by each isomer of Gd**4** are of comparable size and that within each the Gd^{3+} chelate has broadly similar freedom of rotation. The difference in relaxivity of the isomers of Gd**4** in micelles can only partially be the result of differences in molecular rotation between the two systems. The major difference between the two profiles again stems from the longer r_{GdH} value found for *S-SSS*-Gd**4**. This is demonstrated by a simulated NMRD profile using the fitting parameters from the profile of *S-RRR*-Gd**4** but employing the hydration parameters from the *SSSS*-Gd**4** profile – τ_M = 8 ns and r_{GdH} = 3.1 Å (dashed line, Figure 4). This simulation accounts for the majority of the relaxivity enhancement observed for *S-RRR*-Gd**4** and indicates that the primary limitation to enhancing relaxivity at high fields for *S-SSS*-Gd**4** is a combination of the longer r_{GdH} value observed for this chelate and a value of τ_M that is rather too short to optimize relaxivity at 20 MHz.

As previously noted the τ_M value of *S-SSS*-Gd**4**, at 8 ns, is somewhat shorter than optimal at 20 MHz, under the traditional SBM paradigm.[10,34] This is reflected in a shift of the maxima of the two relaxivity 'humps' in the NMRD profiles shown in Figure 4. The more rapidly exchanging *S-SSS*-Gd**4** exhibits a 'hump' maximum that is at 10 to 20 MHz higher field than the more slowly exchanging *S-RRR*-Gd**4**, consistent with expectation based on the different water exchange kinetics of the two isomers. However, it is important to note that even at the higher fields where the exchange rate of *S-SSS*-Gd**4** would be considered optimal the relaxivity of *SRRR*-Gd**4** remains higher and this must be a direct result of the increase in r_{GdH}.[10,34]

Interactions of biphenyl conjugates with poly-β-cyclodextrin

Hydrophobic groups such as the aromatic substituent of Gd**4** are known to form inclusion compounds with β-cyclodextrin (β-CD). Cyclodextrins themselves are not sufficiently large to slow rotation to the extent that substantial gains in relaxivity can be realized, but polymers of cyclodextrins are large enough and have previously been used to slow molecular tumbling and increase relaxivity.[68-70] Poly-β-cyclodextrin (poly-β-CD) contains an average of 10 - 11 β-CD units, each of which can bind and slow the tumbling of Gd**4**. The advantage of this approach is that, unlike the serum albumin binding described below, poly-β-CD affords only approximately equivalent binding sites and will slow the rotation of each chelate it binds approximately equivalently. In consequence, the binding of Gd**4** to poly-β-CD conforms, to a first approximation, to a simple 1:1 binding model. Titrating a dilute solution of Gd**4** with poly-β-CD and measuring the change in water proton relaxation rate affords typical binding curves for both isomers of Gd**4** (Figure 5). The increase in water proton relaxation rate as Gd**4** is added to poly-β-CD is a clear indication of a reduction in the rate of molecular tumbling of the Gd^{3+} chelates (longer τ_R) as the chelates bind to the polymer. The data were fitted to a simple model that considers the presence of 11 equivalent and independent binding sites, affording association constants and bound relaxivities (r_1^{bound}) for the two isomeric chelates (Table 3).

The association constants determined in this way (Table 3) are probably a good reflection of the strength of the interaction between each isomer of Gd**4** and a β-CD unit. Although these values are an average over all β-CD of the polymer there is no reason to suppose that the binding of one chelate by poly-β-CD will substantially change the binding of any of the others and each binding site must be very similar, if subtly different. The binding of *S-SSS*-Gd**4** to β-CD is somewhat stronger than that of *S-RRR*-Gd**4** even though the same group is responsible for binding in each case. Since these are interactions between chiral host and chiral guest in each case, differences in the binding of the two isomers were expected. The results of molecular modelling studies (below) further highlight how these differences in interaction are likely to occur. Unlike K_a, the relaxivity of Gd**4** bound to poly-β-CD is expected to vary somewhat depending on the location of the β-CD unit in the polymer – chelates bound closer to the middle of the molecular assembly could reasonably be assumed to have less (or at least slower) motion of rotation than those closer to the ends. In this light it is important to treat r_1^{bound} values as averaged values rather than absolute values for a discrete chelate. Nonetheless, this exercise is highly instructive; the bound relaxivity (Table 3) of the more rapidly exchanging TSAP isomer again has lower value than the more slowly exchanging SAP isomer when molecular tumbling is slowed.

NMRD profiles of the two isomers of Gd**4** were recorded under conditions that ensured > 96 % of the chelate was bound to poly-β-CD (Figure 6). Again only the high field region of the profiles are shown and fitted. Notably the two profiles closely resemble those obtained for the chelates in micelles. Fitting the profiles to SBM theory (including the Lipari-Szabo model) affords similar rotational correlation times, τ_g and τ_l, for the two isomers of Gd**4** bound to poly-β-CD (Table 4) indicating that differences in molecular tumbling between the two isomers are not the primary cause of the difference in relaxivity. Yet again it is found that the critical impact of the longer r_{GdH} value of *S-SSS*-Gd**4** is the primary cause of the lower relaxivity observed for the more rapidly exchanging TSAP isomer. A profile simulated with fitting parameters for *SSSS*-Gd**4**, but using the water exchange parameters for *S-RRR*-Gd**4**, accounts for all of the difference between the profiles at the high and low field regions of the relaxivity ‘hump’ and most (about 80%) of the ‘hump’ around 20 MHz (dashed line, Figure 6). The remaining differences in relaxivity may be attributed to the small differences that exist between the local rotations (τ_l) of the two chelates when bound to poly-β-CD. The relaxivity maximum observed for each chelate exhibits the same field

dependence as observed in the micelle system – the more rapidly exchanging isomer peaking at higher field – consistent with expectation.

Interactions of biphenyl conjugates with Human Serum Albumin

Titrating human serum albumin (HSA) into dilute solutions of Gd**4** below the cmc clearly demonstrates the relaxivity enhancement afforded by the interaction of the Gd^{3+} chelate with the protein (Figure 7). As the amount of HSA present increases the relaxivity of each chelate increases as the chelate binds to the protein and molecular tumbling is slowed. However, unlike poly-β-CD with its approximately equivalent binding sites, HSA has multiple, very different hydrophobic binding sites and is capable of binding a large number of hydrophobic molecules simultaneously. Because chelate binding in proteins such as HSA is allosteric, the binding of Gd**4** at any given site alters the chelate-protein interaction at all other binding sites. As a consequence, fitting this type of titration data does not provide information with true *physical* meaning about the agent, its binding or relaxivity. A binding model incorporating 3 equivalent binding sites on the protein describes the data for each chelate quite well and allows a *qualitative* assessment of the titration data in Table 5. From the inflection of the binding curve which occurs significantly before a 1:1 stoichiometry it is clear that both chelates bind reasonably avidly to more than one site on the protein, justifying the use a 3:1 binding model. The overall binding affinity of *S-RRR*-Gd**4** appears to be higher than that of *S-SSS*-Gd**4**. Furthermore, the effect of the longer r_{GdH} value for *S-SSS*-Gd**4** is again evident as its relaxivity is evidently lower than that of *S-RRR*-Gd**4**.

Relaxometric titrations cannot discriminate between chelates bound to different sites on the protein and it is highly unlikely that either chelate is able to find three equivalent sites at which to bind. To probe the binding interactions in more depth site specific binding assays are required. The work of Sudlow and co-workers[71,72] has provided a great deal of information about the binding interactions of HSA as well as methods for probing these interactions. Caravan and co-workers employed those methods to probe the interactions of the clinical blood pool agent MS-325.[73] Given the well-developed nature of this experimental protocol identical techniques were used to probe the binding of each isomer of Gd**4** to HSA. A fluorescent probe specific for a particular biding site on HSA was added to a solution of defatted HSA and its displacement by Gd**4** followed by fluorescence. Warfarin is a probe that is known to selectively bind in what Sudlow designated drug binding site I.[71] When either isomer of Gd**4** was titrated into the solution no displacement of warfarin from HSA was observed (Supplementary Information, S4). This appears to indicate that there is no binding of either isomer at this site; however, drug binding site I is a very large binding domain and three distinct subdomains: a, b and c; have been noted within drug binding site I.[74] Warfarin binds in subdomain Ia which is the subdomain located closest to the mouth of the binding pocket and between subdomains Ib and Ic. When bound, warfarin is known to extend partially into both subdomains Ib and Ic, and therefore binding of Gd**4** in either subdomain Ib or Ic was expected to lead to at least partial displacement of warfarin from drug binding site I. In light of the results from the relaxometric titrations the possibility that drug binding site I is able to accommodate Gd**4** and warfarin simultaneously, without displacement of warfarin, cannot be excluded. Indeed the results of molecular modelling studies (below) suggest that from an energetic perspective binding of the chelates in this site remains a possibility. In contrast dansyl sarcosine binds selectively in what Sudlow designated drug binding site II.[71] Gd^{3+} chelates, including the clinical HSA binders MS.325 and GdBOPTA, are often found to bind in drug binding site II. Perhaps not unexpectedly then addition of either isomer of Gd**4** resulted in displacement of the dansyl sarcosine causing a decrease in emission intensity (Supplementary Information, S4). Following the methods of Caravan and co-workers, inhibition constants for the fluorescent probe at drug binding site II can be determined for each isomer from which the strength of each

association can be calculated (Table 6). The association constants determined in this way are of a similar magnitude to that observed for MS-325. Notably the two isomers have quite different association constants for binding at drug binding site II but these results are in contradiction to those obtained from the relaxometric titration (Figure 7). The binding of *S-RRR*-Gd**4**, globally stronger from the relaxometric titration, is the weaker of the two isomers at drug binding site II. Two factors could contribute to this difference. Firstly, *S-RRR*-Gd**4** could either be binding more strongly to other sites or binding to more sites on HSA – the results of molecular modelling studies (below) suggest that even drug binding site I could be occupied by this chelate. Secondly, the apparent r_1^{bound} value determined from the relaxometric titration (Table 5), as noted previously, has no physical relation to the behavior of any single chelate molecule. This value is a weighted average over chelate bound to all sites, none of which are expected to have identical relaxivities, and the model allows for only three bound chelates when in fact there could be many more. As a result, this parameter may easily be an underestimate, and if this were indeed the case then the value of the association constants determined from the fitting would tend to be overestimated.

NMRD profiles were collected for both isomers under conditions designed to maximize the amount of Gd**4** bound to HSA (Figure 8). Conditions were chosen under which >99% of each isomer of Gd**4** is estimated to be globally bound to HSA, respectively (80 and 85 % bound to site II, respectively, on the basis of the displacement experiments). Given the distribution of environments in which Gd**4** could be found in these systems any NMRD fitting is without meaning and thus none was attempted. The same overall pattern is observed as for the other slowly tumbling systems studied herein. High field relaxivity 'humps' are again observed for both chelates but the 'hump' maximum observed for *S-RRR*-Gd**4** is significantly higher than that of *S-SSS*-Gd**4**. This can again be attributed to the difference metal-water distance, r_{GdH}, between the two isomeric chelates. On the higher field edge of the 'hump' the relaxivity of both agents falls off quickly, consistent with theory. It is evident that the relaxivity of *S-RRR*-Gd**4** falls off more quickly than that of *S-SSS*-Gd**4** until, at around 40 MHz, it falls below that of *S-SSS*-Gd**4**. This observation is expected on the basis of the previously determined dissociative water exchange rates of each chelate; that determined for *S-SSS*-Gd**4** being more suitable for achieving higher relaxivities at higher fields, according to the traditional SBM paradigm.[10,34]

Variable temperature relaxometry and molecular modelling studies

One key assumption has been made in the analysis of all the relaxivity measurements herein: the water exchange kinetics of both chelates remains virtually unaffected by the interactions that slow the global rate of molecular tumbling. This is a point of particular relevance when considering the agents bound to HSA as it has previously been reported that the interaction of a chelate with the protein can affect its water exchange kinetics.[73,75-77] The water exchange kinetics of Gd^{3+} chelates are accurately determined by measuring the effect of changing temperature on the ^{17}O transverse relaxation rate of water in a solution of the chelate.[78,79] The water exchange kinetics of the two isomeric Gd**1** chelates were determined using this method.[34] The limitation of this technique is that it requires relatively high concentrations of Gd^{3+} (typically 10^{-2} M), much higher than the limits of solubility of HSA or poly-β-CD. Samples cannot then be prepared in which sufficient chelate is present in solution under conditions where the majority of the chelate is bound to the macromolecule. The water exchange kinetics of the bound chelate cannot therefore be determined in this manner. Caravan and co-workers proposed a method by which absolute quantification of water exchange kinetics could be achieved from variable temperature ^1H relaxation measurements at much lower chelate concentrations using the corresponding Dy^{3+} chelate.[75] It is generally considered that Ln^{3+} ions may be interchanged to afford differing types of information that build up a picture of the overall coordination chemistry – as noted earlier

where the Eu^{3+} chelate was studied to probe hydration equilibria. However, in our case there are concerns that switching to a heavier Ln^{3+} ion (rather than the lighter Eu^{3+} ion) will bring the TSAP isomer closer to a tipping point at which the hydration state of the chelates in the TSAP coordination geometry are thought to abruptly begin to decrease. Dy^{3+} is adjacent to Ho^{3+} in the lanthanide series and from recent crystallographic data on a TSAP Ho^{3+} chelate it is evident that the hydration equilibrium of a TSAP Ho^{3+} chelate in solution is complex indeed.[80] The extent to which the hydration and exchange kinetics of a TSAP Dy^{3+} chelate can be said to reflect those of a TSAP Gd^{3+}, with its much simpler hydration behaviour, is highly questionable. For this reason we took two different approaches to assess the likelihood of changes in water exchange kinetics as the rate of molecular tumbling is slowed.

Firstly, molecular models were used to examine the orientation of the chelates when bound to the macromolecules HSA and poly-β-CD. The results of modelling the interactions between Gd**4** and β-CD suggest very similar interactions for both isomeric chelates (interaction energies of −24.4 ±1.4 kcal/mol and −25.7 ± 0.8 kcal/mol for the *S-RRR*-Gd**4** and *S-SSS*-Gd**4**, respectively), consistent with the experimentally determined association constants. The orientation of each isomeric chelate when bound to a β-CD unit (Figure 9) may help explain the observed differences in the K_a for the two chelates. From the molecular models it is clear that in each case the biphenyl group extends right through the cyclodextrin binding pocket and it is the *para*- substituted phenyl and thiourea group that are held in the binding cavity. Binding is thus the result of hydrophobic interactions between the phenyl group and the inner surface of the cavity and hydrogen bonding interactions between the thiourea group and the primary hydroxyl groups on the narrow rim. This binding mode brings the chiral chelate in close proximity to the wider rim of the β-CD cavity. β-CD interacts stereoselectively with chiral compounds[81] and here the secondary hydroxyl groups of the wider rim will interact differently with the chelates' pendant arms depending upon their orientation (either Λ or Δ). In each case the hydrophobic substituent is located on the corner of the macrocycle (Figure 1) which orients the water coordination site such that it will rotate pointing up and away from the β-CD unit, into the bulk water. It would be expected that such an orientation would minimize interference in the water exchange process of both isomers of Gd**4** when bound to poly-β-CD. We may reasonably assume that binding of Gd**4** to β-CD does not significantly influence the rate of water exchange in either chelate – any influence from this binding can reasonably be assumed to be very similar for each isomeric chelate.

Although experimentally no displacement of warfarin was observed, molecular modelling studies suggest that both isomers of Gd**4** are capable of binding in drug binding site I (Figure 10). They would need to be capable of doing so without displacing warfarin and it is possible to model the docking of both isomers Gd**4** in such a way as to accommodate both Gd**4** and warfarin in the binding pocket. This is possibility arises only because the binding pocket of drug binding site I is so large that accommodation of the Gd^{3+} chelate simultaneously with the fluorescent probe is possible.[54] Despite the size of this binding pocket, docking calculations show the biphenyl groups held in the binding pocket with the chelates held at some distance away from the mouth of the pocket by the *para*-phenyl linker. This suggests a considerable degree of freedom of motion on the part of the chelate end of the molecule. Although the calculated docking modes orient the water binding face of the isomeric chelates in different directions relative to the protein surface, they are both pointing essentially outward towards the bulk water. It is important to bear in mind that these are single low energy minima of the chelate positions and are not a reflection of the time-averaged orientation of the water binding face. Given the apparent freedom of motion of each chelate when bound to HSA it seems unlikely that the exchangeable water molecule of

either chelate is constrained to face towards the protein surface which could result in an apparent deceleration of water exchange.

Both isomers of Gd**4** are experimentally found to bind to drug binding site II of HSA (Table 6). Docking calculations position *S-SSS*-Gd**4** more deeply in the pocket than *S-RRR*-Gd**4**, this permits the thiourea to engage the side chain of Ser489 in hydrogen bonding interactions (Figure 10). Such a difference in binding mode may have a significant impact on the freedom of local rotation of the two chelates. The chelate of *S-SSS*-Gd**4** will be held more closely to the surface of the protein which may reasonably be presumed to reduce local rotation of the chelate. This would tend to increase relaxivity. However, the difference in binding mode provides no reason to suppose that the water exchange rate of either chelate would be affected by this binding. Both chelates will rotate locally around a point of attachment (the corner of the macrocycle) which would seem to maintain the water coordination site of each isomer pointing away from the protein surface and into the bulk. These results may account for the stronger binding interactions observed for the *S-SSS*-Gd**4**.

In a qualitative sense the accuracy of the binding predictions that come out of these modelling exercises can be tested through variable temperature ^{1}H relaxation measurements. Since a number of parameters that are temperature dependent controls relaxivity, the temperature profile of relaxivity can be very informative. This is of particular relevance here since τ_M has a non-negligible effect upon the characteristic correlation time τ_C (equation 3) when τ_R is long, *i.e.* in a slowly rotating system. Furthermore, τ_M is a primary determinant of the effectiveness of the transfer of the paramagnetic effect to the bulk (equation 1).

From the Solomon-Bloembergen.Morgan equations (eqns 1-3) two limiting cases for inner-sphere relaxivity (r_1^{is}) may be defined:

The fast exchange regime, $\tau_M < T_{1M}$. For low molecular weight Gd^{3+} chelates this condition typically occurs when $\tau^{298}_M < 100 – 200$ ns.

The slow/intermediate regime, $\tau_M \geq T_{1M}$. In this regime the rate of water exchange is so slow that the condition $\tau_M > T_{1M}$ occurs over an extended temperatures range.

In the fast exchange regime T_{1M} is the primary determinant of inner-sphere relaxivity. At low temperatures τ_R and $T_{1,2e}$, and therefore τ_C, are long. The result is that T_{1M} shortens with decreasing temperature causing relaxivity to rise with decreasing temperature. In slowly tumbling macromolecular systems the values of T_{1M} are also shorter and the fast exchange regime is not reached until $\tau_M^{298} < 30$ ns. In the slow/intermediate exchange regime inner-sphere relaxivity decreases with decreasing temperature and eventually tends towards zero, following the increase of the water exchange lifetime.

The temperature relaxivity profiles of each isomer of Gd**4** were recorded under three of the molecular tumbling regimes described herein: as discrete chelates below the cmc; when bound to poly-β-CD; and when bound to HSA (Figure 11). The temperature response of the relaxivity of the discrete chelates (Figure 11a) reflects the known difference in water exchange kinetics between the two isomeric chelates. At room temperature and above both chelates are in fast-exchange regime and their relaxivity decreases exponentially with temperature. As temperature dips below about 15 °C the behavior of the two chelates begins to deviate: while *S-SSS*-Gd**4** remains in the fast exchange regime, for *S-RRR*-Gd**4** the value of τ_M becomes so long as the temperature continues to drop that the chelate drops out of the fast exchange regime and relaxivity begins to flatten out, eventually dropping below that of *S-SSS*-Gd**4**. These temperature profiles can be fitted in terms of the parameters $\Delta H_i^{\#}$ (i = M, V, R, D) using the best-fit parameters from Table 2, and assuming an Eyring-type behaviour for the parameters τ_R, τ_M, τ_V and D (the relative diffusion coefficient of solvent and Gd^{3+}

chelate). This procedure affords excellent fits that strongly support the previously determined values of the τ_M values for the two Gd**4** isomers.[34]

In the two slowly tumbling systems (Figure 11b and c) the relaxivity of *S-SSS*-Gd**4** exhibits an increase in relaxivity with decreasing temperature similar to that observed for the discrete chelates; indicating that the chelate remains in the fast exchange regime throughout. In contrast, the relaxivity of *S-RRR*-Gd**4** decreases with decreasing temperatures indicating that the water exchange is slower. The decrease in T_{1M} arising from slower molecular tumbling drives the chelate into a slow/intermediate exchange regime. Notably, in each profile there is a single temperature at which the relaxivity of the two isomers are equal and this temperature increases as the system rotated more slowly, reflecting the effect of decreasing T_{1M} on *S-RRR*-Gd**4** in the slow/intermediate exchange regime. What these data show is that the relative rates of water exchange of the two isomers remain consistent across the systems studied herein: *S-RRR*-Gd**4** is a more slowly (but still rapidly) exchanging chelate and *S-SSS*-Gd**4** a more rapidly exchanging chelate in all these systems and binding of these agents to either poly-β-CD and HSA does not affect this situation.

Conclusions

Conventional wisdom in the field of contrast agent development has held that in order to maximize relaxivity it is necessary to make two modifications to the low molecular weight Gd^{3+} chelate currently employed in this role. First, the chelate must be prevented from tumbling rapidly in solution, such that $\tau_R > 1$ ns or so. Secondly, water exchange must be accelerated to some optimal value, such that $\tau_M < 20$ ns. While it is undeniably the case that slow molecular tumbling and fast water exchange hold the key to the highest relaxivities, the results presented herein show that conventional wisdom doesn't have it quite right. Preparing two isomeric Gd^{3+} chelates with very similar electronic relaxation properties but very different dissociative water exchange kinetics afforded the opportunity to undertake a direct side-by side comparison of the effect of changing water exchange kinetics on relaxivity. Theory indicates that one chelate should have had vastly superior relaxivity: that should have been the one that exchanged water most rapidly (the TSAP isomer). Instead what we observe is that the more slowly exchanging actually has substantially higher relaxivity. Analysis of the relaxometric data reveals that the origin of this unique and unexpected result lies in a difference in hydration state (q/r_{GdH}^6) between the two isomers. The lower hydration state of the rapidly exchanging TSAP isomer and has a profoundly limiting effect on relaxivity. These results demonstrate that far from being a matter of little importance, the hydration state (number and position of water molecules in the inner coordination sphere) can have a very profound effect on relaxivity. This demonstrates that, contrary to the commonly performed superficial analyses of theory, simply ‘optimizing’ water exchange in Gd^{3+} chelates is no guarantee that very high relaxivities will be attained.

Experimental

General Remarks

All solvents and reagents were purchased from commercial sources and used as received. HPLC purifications were performed on a Waters δ-Prep 150 HPLC system using a Phenomenex Luna C-18 reversed-phase (50 × 250 mm) column. In all cases absorbance was monitored at 205 and 254 nm. The solvent system employed for the purification of chelates eluted with water (0.037 % HCl) for 5 minutes and then with a linear gradient to 80 % MeCN and 20 % water (0.037% HCl) after 40 minutes, at a flow rate of 50 $mLmin^{-1}$. ^1H and ^{13}C NMR spectra were recorded on a JEOL Eclipse 270 spectrometer at 270.17 MHz and 67.93 MHz, respectively or on a Varian Mercury 300 spectrometer operating at 300.01 MHz and 75.47 MHz, respectively. The $1/T_1$ nuclear magnetic relaxation dispersion profiles

of water protons were measured over a continuum of magnetic field strength from 0.00024 to 0.5 T (corresponding to 0.01 – 20 MHz proton Larmor frequency) on the fast field-cycling Stelar Spinmaster FFC 2000 relaxometer equipped with a silver magnet. The relaxometer operates under complete computer control with an absolute uncertainty in the $1/T_1$ values of ± 1%. The typical field sequences used were the NP sequence between 40 and 8 MHz and PP sequence between 8 and 0.01MHz. The observation field was set at 13 MHz. 16 experiments of 2 scans were used for the T_1 determination for each field. Additional data at higher fields (30 - 70 MHz) were measured on a Stelar Spinmaster relaxometer equipped with a Bruker electromagnet operating in the range 20 to 80 MHz. The synthesis of the ligands *S-SSS*-**2** and *S-RRR*-**2** have been reported previously.[34]

(4*S*,7*S*,10*S*)–α,α',α''-Trimethyl-[(*S*)-2-(4-aminobenzyl)]-1,4,7,10-tetraazacyclododecane-1,4,7,10-tetraacetic acid (*S-SSS*-2)

The nitrobenzyl ligand *S-SSS*-**1** (125 mg, 0.187 mmol) was dissolved in water (10 mL) and 10 % palladium on carbon (20 mg) was added. The reaction mixture was shaken on a Parr Hydrogenator apparatus for 12 h under H_2 (25 psi). The catalyst was removed by filtration and the solvents lyophilized to afford the title compound as a colourless solid (111 mg, 94 %).

^{1}H NMR (300 MHz, D_2O pD 7), δ = 6.84 (2H, d, $^3J_{H\text{-}H}$ = 7 Hz, Ar), 6.62 (2H, d, $^3J_{H\text{-}H}$ = 7 Hz, Ar), 1.7-3.5 (22H, m br), 0.98 (9H, m, CH_3); ^{13}C NMR (75.5 MHz, D_2O pD 7), δ = 7.3 (CH_3), 7.5 (CH_3), 7.7 (CH_3), 43.3, 45.1, 45.2, 46.9, 47.2, 47.4, 54.8, 56.9, 57.9, 58.0, 58.2, 58.5, 59.8, 116.8 (Ar), 130.1 (Ar), 131.5 (Ar), 144.2 (Ar), 182.3 (CO_2), 182.6 (CO_2), 182.7 (CO_2), 182.8 (CO_2); m/z (ESMS ESI+): 590 (8 %, $[H_4L + K]^+$), 612 (55 %, $[NaH_3L + K]^+$), 634 (71 %, $[Na_2H_2L + K]^+$), 656 (100 %, $[Na_3HL + K]^+$); ν_{max} / cm^{-1} (ATR / pH 7): 3338 (NH), 2968, 2829, 1573 (CO_2), 1462, 1408, 1258, 1227, 1166, 1126, 1032.

(4*R*,7*R*,10*R*)–α,α',α''-Trimethyl-[(*S*)-2-(4-aminobenzyl)]-1,4,7,10-tetraazacyclododecane-1,4,7,10-tetraacetic acid (*S*-RRR-2)

The title compound was prepared from *S-RRR*-**1** according to the procedure employed for *S-SSS*-**2** and was isolated after removal of the solvents by lyopholization to afford a pale yellow solid (156 mg, 92 %).

^{1}H NMR (300 MHz, D_2O pD 2), δ = 7.23 (4H, m, Ar), 2.6-4.1 (22 H, m br), 1.30 (9 H, m, CH_3); ^{13}C NMR (75.5 MHz, D_2O pD 2), δ = 13.6 (2 × CH_3), 14.5 (CH_3), 31.7, 32.4, 46.7 (br), 49.3 (br), 51.8, 53.4, 57.8, 58.7, 59.8, 61.6, 62.4 123.6 (Ar), 128.9 (Ar), 131.2 (Ar), 138.1 (Ar), 172.1 (2 × C=O), 175.1 (C=O), 176.0 (C=O); m/z (ESMS ESI+): 552 (83 %, $[H_4L+H]^+$), 574 (45%, $[H_4L + Na]^+$) 590 (100 %, $[H_4L + K]^+$); ν_{max} / cm^{-1} (ATR / pH 2): 3333 (NH), 2842, 2569, 1713 (CO_2H), 1620, 15556, 1540, 1506, 1473, 1455, 1207, 1163, 1099.

(4*S*,7*S*,10*S*)–α,α',α''-Trimethyl-[(*S*)-2-(4-isothiocyanatobenzyl)]-1,4,7,10-tetraazacyclododecane-1,4,7,10-tetraacetic acid (*S-SSS*-3)

The amine *S-SSS*-**2** (108 mg, 0.170 mmol) was dissolved in water (4 mL) and the pH of the resulting solution adjusted to 2 by addition of a dilute HCl solution. Chloroform (6 mL) was added to the reaction which was then stirred vigorously at room temperature. Thiophosgene (68 mg, 0.59 mmol) was added to the reaction which was then stoppered and stirred vigorously for 18 hours at room temperature. The reaction mixture was then transferred to a separatory funnel and the chloroform layer was allowed to run off. The aqueous layer was then washed with chloroform (2 × 15 mL). The aqueous layer was then collected and the

solvents removed under reduced pressure to afford the title compound as a colourless solid (111 mg, 95 %).

^{1}H NMR (300 MHz, D_2O), δ = 7.35 (4H, m, Ar), 2.6 - 4.6 (22H, m br), 1.61 (3H, s br, CHC$\underline{H}_3$), 1.50 (3H, s br, CHC$\underline{H}_3$), 1.33 (3H, s br, CHC$\underline{H}_3$); m/z (ESMS ESI+): 594 (39 %, $[M+H]^+$), 616 (100 %, $[M+Na]^+$), 532 (10 %, $[M+K]^+$); ν_{max} / cm^{-1}: 3345 (OH), 2986, 2102 (SCN), 1722 (C=O), 1516, 1455, 1394 1222, 1160, 1102, 1027; Anal. Found C = 44.8 %, H = 6.3 %, N = 9.7 %, $C_{27}H_{39}N_5O_9S{\cdot}3(H_2O){\cdot}2(HCl)$ requires C = 45.0 % H = 6.6 % N = 9.7 %.

(4*R*,7*R*,10*R*)–α,α',α''-Trimethyl-[(*S*)-2-(4-isothiocyanatobenzyl)]-1,4,7,10-tetraazacyclododecane-1,4,7,10-tetraacetic acid (*S*-*RRR*-3)

The title compound was prepared from *S*-*RRR*-**2** according to the procedure employed for *S*-*SSS*-**3** and was isolated after removal of the solvents removed under reduced pressure to afford a colourless solid (127 mg, 93 %).

^{1}H NMR (300 MHz, D_2O), δ = 7.15 (4H, m, Ar), 2.5-4.4 (22H, m br), 1.34 (9H, m, CH_3); m/z (ESMS ESI.): 592 (100 %, $[M-H]^-$); ν_{max} / cm^{-1}: 2924, 2098 (SCN), 1716 (C=O), 1558, 1520, 1506, 1456, 1394, 1204, 1097.

(4*S*,7*S*,10*S*)–α,α',α''-Trimethyl-[(S)-2-(4-[3-(biphenyl-4-ylmethyl)thioureido]phenyl methyl)]-1,4,7,10-tetraazacyclododecane-1,4,7,10-tetraacetate gadolinium(III) chelate (H[Gd(*S*-*SSS*-4)])

The isothiocyanate *S*-*SSS*-**3** (102 mg, 0.150 mmol) was dissolved in water (5 mL) and the pH of the solution adjusted to 8 (1M NaOH solution). The solution was stirred at room temperature and a solution of 4-phenylbenzylamine (38 mg, 0.21 mmol) in dioxane (5 mL) was added. The reaction mixture was stirred at room temperature for 18 hours. A solution of gadolinium chloride hexahydrate (64 mg, 0.17 mmol) in water (2 mL) was then added to the reaction, the pH being maintained at 6 by periodic addition of a 1 M solution of NaOH. The reaction was stirred at room temperature for 48 hours. The solvents were removed *in vacuo* and the residue dissolved in a mixture of water and THF prior to HPLC purification. After removal of the HPLC eluent by lyophilisation the title compound was obtained as a colourless solid (58 mg, 43%).

HPLC R_T = 32.77 min; m/z (ESMS ESI−): 930 (100 %, $[GdL]^-$), the appropriate isotope pattern was observed; Anal. Found C = 46.9 %, H = 6.0 %, N = 8.0 %, $C_{40}H_{49}N_6O_8SGd{\cdot}5(H_2O)$ requires C = 47.0 % H = 5.8 % N = 8.2 %.

(4*R*,7*R*,10*R*)–α,α',α''-Trimethyl-[(*S*)-2-(4-[3-(biphenyl-4-ylmethyl)thioureido]phenyl methyl)]-1,4,7,10-tetraazacyclododecane-1,4,7,10-tetraacetate gadolinium(III) chelate (H[Gd(*S*-*RRR*-4)])

The title compound was prepared from *S*-*RRR*-**3** according to the procedure employed for Gd*S*-*SSS*-**4** and was isolated after removal of the solvents by lyophilisation to afford a colourless solid (49 mg, 39%).

HPLC R_T = 31.55 min; m/z (ESMS ESI−): 930 (100 %, $[GdL]^-$), the appropriate isotope pattern was observed

(4*S*,7*S*,10*S*)–α,α',α''-Trimethyl-[(*S*)-2-(4-[3-(biphenyl-4-ylmethyl)thioureido]phenyl methyl)]-1,4,7,10-tetraazacyclododecane-1,4,7,10-tetraacetate europium(III) chelate (H[Eu(*S*-*SSS*-4)])

The title compound was prepared from *S*-*SSS*-**3** and europium chloride hexahydrate according to the procedure employed for Gd*S*-*SSS*-**4** and was isolated after removal of the solvents by lyophilisation to afford a colourless solid (52 mg, 40%).

HPLC R_T = 33.73 min; ^{1}H NMR (300 MHz, D_2O), δ = 18.97 (NCH_2-H_{ax}), 17.93 (2H, NCH_2-H_{ax}), 17.20 (NCH_2-H_{ax}), 8.35 – 6.0 (17H, m br, Ar and C$\underline{H}_2$Ar), 0.77 (NCH_2-H_{eq}), 0.84 (2H, NCH_2-H_{eq}), −0.56 (CH_3), −1.11 (NCH_2-H_{eq}), −2.06 (CH_3), −2.36 (NCH_2-H_{ax}), −2.74 (NCH_2-H_{ax}), −3.04 (CH_3), −3.99 (NCH_2-H_{ax}), −4.76 (NCH_2-H_{ax}), −5.18 (2H, NCH_2-H_{eq}) –5.48 (NCH_2-H_{eq}), −6.69 (H_{ac}), −7.14 (H_{ac}), −7.84 (H_{ac}), −9.73 (H_{ac}), −11.57 (H_{ac}); m/z (ESMS ESI−): 925 (100 %, $[EuL]^-$), the appropriate isotope pattern was observed; Anal. Found C = 41.5 %, H = 5.5 %, N = 7.1 %, $C_{40}H_{48}N_6O_8SEuNa{\cdot}11(H_2O)$ requires C = 41.9 % H = 6.1 % N = 7.3 %.

(4*R*,7*R*,10*R*)–α,α',α''-Trimethyl-[(*S*)-2-(4-[3-(biphenyl-4-ylmethyl)thioureido]phenyl methyl)]-1,4,7,10-tetraazacyclododecane-1,4,7,10-tetraacetate europium(III) chelate (H[Eu(*S*-*RRR*-4)])

The title compound was prepared from *S*-*RRR*-**3** and europium chloride hexahydrate according to the procedure employed for Gd*S*-*SSS*-**4** and was isolated after removal of the solvents by lyophilisation to afford a colourless solid (44 mg, 37%).

HPLC R_T = 32.23 min; ^{1}H NMR (300 MHz, D_2O), δ = 37.99 (NCH_2-H_{ax}), 36.20 (NCH_2-H_{ax}), 35.55 (NCH_2-H_{ax}), 35.34 (NCH_2-H_{ax}), 11.59 (1H, d, $^2J_{H\text{-}H}$ 7 Hz, NCHC$\underline{H}_2$Ar), 9.74 (1H, d, $^2J_{H\text{-}H}$ 7 Hz, NCHC$\underline{H}_2$Ar), 8.45 (2H, aa′, $^2J_{H\text{-}H}$ 13 Hz, NHC$\underline{H}_2$Ar), 7.80 (3H, m, Ar), 7.76 (2H, d, $^3J_{H\text{-}H}$ 8 Hz, *para*-substituted Ar), 7.67 (2H, t, $^3J_{H\text{-}H}$ 7 Hz, Ar), 7.44 (2H, d, $^3J_{H\text{-}H}$ 8 Hz, *para*-substituted Ar), 7.24 (2H, d, $^3J_{H\text{-}H}$ 8 Hz, *para*-substituted Ar), 7.03 (2H, d, $^3J_{H\text{-}H}$ 8 Hz, *para*-substituted Ar), 1.51 (NCH_2-H_{eq}), 0.78 (NCH_2-H_{eq}), 0.27 (NCH_2-H_{eq}), −1.02 (NCH_2-H_{eq}), −2.92 (CH_3), −3.73 (CH_3), −4.05 (CH_3), −5.80 (NCH_2-H_{ax}), −6.06 (NCH_2-H_{ax}), −6.97 (NCH_2-H_{ax}), −7.66 (2H, NCH_2−H_{ax} and NCH_2-H_{eq}), −9.90 (NCH_2-H_{eq}), −11.37 (NCH_2-H_{eq}), −12.70 (H_{ac}), −14.64 (H_{ac}), −19.50 (H_{ac}), −20.17 (H_{ac}), −20.31 (H_{ac}); m/z (ESMS ESI−): 925 (100 %, [EuL]−), the appropriate isotope pattern was observed.

Molecular Modelling—All modelling and docking procedures were carried out using the MOE molecular modelling package (MOE Version 2004.03 Chemical Computing Group Inc. Montreal, Canada). The structures of the chelates of Gd**4** were built from the crystal structure of the DOTA-type chelates obtained from the Cambridge Structural Database (entry code JOPJIH; www.ccdc.cam.ac.uk/) and modelled using the Moe-Builder module keeping the Gd^{3+} coordination cage fixed. Conformational analysis of the isomeric Gd**4** chelates was performed by a simulated annealing molecular dynamics (SAMD) method. High-temperature MD calculations were carried out at 1000 K with the starting velocities calculated from the Boltzmann distribution. Each simulation ran for 2000 ps in steps of 0.1 fs with coordinates saved every 2 ps resulting in 1000 conformations. Each conformation was subject to an energy-minimization step until 0.01 convergence and then to a second molecular dynamic at 300 K for 20 interations, followed by conjugate gradient energy minimization until a convergence of 0.001. Clustering of conformations was performed by considering two identical conformers when their difference in energy was below 1 kcal mol^{-1} and their RMSD less than 3.0 Å. The structure of β-CD was taken from the CSD (entry code BCDEXD10). The high-resolution three-dimensional coordinates of human serum albumin (HSA) was obtained from the Protein Data Bank (PDB code 1E7H). Prior to

docking calculations the structures of HSA and β-CD were prepared by adding hydrogen atoms and completing missing atoms. The starting positions for the docking procedure were obtained by modifying the ligand positions and orientations to optimize binding geometry while filling the available space in the HSA drug sites I and II and in the β-CD cavity. Minimization was achieved by a multistep procedure, until convergence was less than 0.01 kcal mol^{-1} $Å^{-1}$. For all calculations a modification of the Amber99 force field[82] was used with in-house parameterization to treat Gd^{3+} chelates within the framework of the ionic method.[50] The docking procedure was performed using the Moe-Dock module with Tabu Search with 10 runs, 1000 steps per run. The ligand binding moiety was kept flexible during the docking calculations. For the β-CD docking the solvent was modelled by using a dielectric constant equal to 20, whereas for the HSA docking an implicit solvation contribution (continuum model) was included to model solvent effects[83] in the docking calculations. The results of the docking calculations were sorted by utilizing a force-field-based scoring function and for each isomer the five best poses were chosen comparing the interaction energies.

Supplementary Material

Refer to Web version on PubMed Central for supplementary material.

Acknowledgments

The authors thank the National Institutes of Health (EB-11687) (MW), Oregon Nanoscience and Microtechnologies Institute (N00014-11-1-0193) (MW), Regione Piemonte (Italy) through the NANO-IGT and Prin 2009 Projects (MB & DL), Portland State University and the Oregon Opportunity for Biomedical Research for financial support of this work, and Drs. Silvio Aime and Enzo Terreno for insightful discussion.

ABBREVIATIONS

DOTA 1,4,7,10-Tetraazacyclododecane-1,4,7,10-tetraacetate

REFERENCES

1. Caravan P, Zhang Z. Eur. J. Inorg. Chem. 2012; 2012:1916. [PubMed: 22745568]
2. Bloembergen N. J. Chem. Phys. 1957; 27:572.
3. Bloembergen N, Morgan LO. J. Chem. Phys. 1961; 34:842.
4. Bloembergen N, Purcell EM, Pound RV. Phys. Rev. 1948; 73:679.
5. Solomon I. Phys. Rev. 1955; 99:559.
6. Solomon I, Bloembergen N. J. Chem. Phys. 1956; 25:261.
7. Caravan P, Ellison JJ, McMurry TJ, Lauffer RB. Chem. Rev. 1999; 99:2293. [PubMed: 11749483]
8. Aime S, Botta M, Fasano M, Terreno E. Chem. Soc. Rev. 1998; 27:19.
9. Botta M, Tei L. Eur. J. Inorg. Chem. 2012; 2012:1945.
10. Lauffer RB. Chem. Rev. 1987; 87:901.
11. Bousquet JC, Saini S, Stark DD, Hahn PF, Nigam M, Wittenberg J, Ferrucci JT. Radiology. 1988; 166:693. [PubMed: 3340763]
12. Sherry AD, Caravan P, Lenkinski Robert E. J. Magn. Reson. Imag. 2009; 30:1240.
13. Kumar K, Jin T, Wang X, Desreux JF, Tweedle MF. Inorg. Chem. 1994; 33:3823.
14. Aime S, Calabi L, Cavallotti C, Gianolio E, Giovenzana GB, Losi P, Maiocchi A, Palmisano G, Sisti M. Inorg. Chem. 2004; 43:7588. [PubMed: 15554621]
15. Werner EJ, Datta A, Jocher CJ, Raymond KN. Angew. Chem., Int. Ed. 2008; 47:8568.
16. Baranyai Z, Botta M, Fekete M, Giovenzana GB, Negri R, Tei L, Platas-Iglesias C. Chem. Eur. J. 2012; 18:7680. [PubMed: 22615142]

17. Cowper SE, Robin HS, Steinberg SM, Su LD, Gupta S, LeBoit PE. Lancet. 2000; 356:1000. [PubMed: 11041404]
18. Grobner T. Nephrol. Dial. Transplant. 2006; 21:1104. [PubMed: 16431890]
19. White Gregory W, Gibby Wendell A, Tweedle Michael F. Invest. Radiol. 2006; 41:272. [PubMed: 16481910]
20. Sarka L, Burai L, Brucher E. Chem. Eur. J. 2000; 6:719. [PubMed: 10807182]
21. Aime S, Caravan P. J Magn Reson Imaging. 2009; 30:1259. [PubMed: 19938038]
22. Baranyai Z, Palinkas Z, Uggeri F, Maiocchi A, Aime S, Brücher E. Chem. Eur. J. 2012
23. Morcos SK, Dawson P. Nephrol. Dial. Transpl. Plus. 2010; 3:501.
24. Rudovsky J, Botta M, Hermann P, Hardcastle KI, Lukeš I, Aime S. Bioconjugate Chem. 2006; 17:975.
25. Benmelouka M, Borel A, Moriggi L, Helm L, Merbach AE. J. Phys. Chem. B. 2007; 111:832. [PubMed: 17249827]
26. Borel A, Bean JF, Clarkson RB, Helm L, Moriggi L, Sherry AD, Woods M. Chem. Eur. J. 2008; 14:2658. [PubMed: 18283704]
27. Senn F, Helm L, Borel A, Daul CA. C. R. Chim. 2012; 15:250.
28. Sherry AD, Brown RD III, Geraldes CFGC, Koenig SH, Kuan KT, Spiller M. Inorg. Chem. 1989; 28:620.
29. Muller RN, Raduchel B, Laurent S, Platzek J, Pierart C, Mareski P, Vander Elst L. Eur. J. Inorg. Chem. 1999:1949.
30. Aime S, Botta M, Parker D, Williams JAG. J. Chem. Soc., Dalton Trans. 1996:17.
31. Beeby A, Clarkson IM, Dickins RS, Faulkner S, Parker D, Royle L, de Sousa AS, Williams JAG, Woods M. J. Chem. Soc., Perkin Trans. 1999; 2:493.
32. Aime S, Botta M, Garda Z, Kucera BE, Tircso G, Young VG, Woods M. Inorg. Chem. 2011; 50:7955. [PubMed: 21819052]
33. Woods M, Aime S, Botta M, Howard JAK, Moloney JM, Navet M, Parker D, Port M, Rousseaux O. J. Am. Chem. Soc. 2000; 122:9781.
34. Woods M, Botta M, Avedano S, Wang J, Sherry AD. Dalton Trans. 2005:3829. [PubMed: 16311635]
35. Caravan P, Astashkin AV, Raitsimring AM. Inorg. Chem. 2003; 42:3972. [PubMed: 12817950]
36. Doble DMJ, Botta M, Wang J, Aime S, Barge A, Raymond KN. J. Am. Chem. Soc. 2001; 123:10758. [PubMed: 11674017]
37. Ruloff R, Toth E, Scopelliti R, Tripier R, Handel H, Merbach AE. Chem. Commun. 2002:2630.
38. Laus S, Ruloff R, Toth E, Merbach AE. Chem. Eur. J. 2003; 9:3555. [PubMed: 12898682]
39. Rudovsky J, Cigler P, Kotek J, Hermann P, Vojtisek P, Lukeš I, Peters JA, Vander Elst L, Muller RN. Chem. Eur. J. 2005; 11:2373. [PubMed: 15685711]
40. Polasek M, Hermann P, Peters JA, Geraldes CFGC, Lukeš I. Bioconjugate Chem. 2009; 20:2142.
41. Rodriguez-Rodriguez A, Esteban-Gomez D, de Blas A, Rodriguez-Blas T, Fekete M, Botta M, Tripier R, Platas-Iglesias C. Inorg. Chem. 2012; 51:2509. [PubMed: 22243216]
42. Woods M, Kovacs Z, Zhang S, Sherry AD. Angew. Chem. Int'l. Ed. 2003; 42:5889.
43. Aime S, Barge A, Bruce JI, Botta M, Howard JAK, Moloney JM, Parker D, de Sousa AS, Woods M. J. Am. Chem. Soc. 1999; 121:5762.
44. Aime S, Botta M, Fasano M, Marques MPM, Geraldes CFGC, Pubanz D, Merbach AE. Inorg. Chem. 1997; 36:2059. [PubMed: 11669824]
45. Howard JAK, Kenwright AM, Moloney JM, Parker D, Woods M, Port M, Navet M, Rousseau O. Chem. Commun. 1998:1381.
46. Woods M, Kovacs Z, Kiraly R, Brücher E, Zhang S, Sherry AD. Inorg. Chem. 2004; 43:2845. [PubMed: 15106971]
47. Webber BC, Woods M. Inorg. Chem. 2012; 51:8576. [PubMed: 22809081]
48. Ruegg CL, Anderson-Berg WT, Brechbiel MW, Mirzadeh S, Gansow OA, Strand M. Cancer Res. 1990; 50:4221. [PubMed: 2364380]

49. Tircso G, Webber BC, Kucera BE, Young VG, Woods M. Inorg. Chem. 2011; 50:7966. [PubMed: 21819053]
50. Gianolio E, Giovenzana GB, Longo D, Longo I, Menegotto I, Aime S. Chem. Eur. J. 2007; 13:5785. [PubMed: 17407109]
51. Schuehle DT, Schatz J, Laurent S, Vander Elst L, Mueller R, Stuart MCA, Peters JA. Chem. Eur. J. 2009; 15:3290. [PubMed: 19206118]
52. Torres S, Martins JA, Andre JP, Geraldes CFGC, Merbach AE, Toth E. Chem. Eur. J. 2006; 12:940. [PubMed: 16224764]
53. Nicolle GM, Toth E, Eisenwiener K-P, Macke HR, Merbach AE. J. Biol. Inorg. Chem. 2002; 7:757. [PubMed: 12203012]
54. Botta M, Avedano S, Giovenzana GB, Lombardi A, Longo D, Cassino C, Tei L, Aime S. Eur. J. Inorg. Chem. 2011:802.
55. Benetollo F, Bombieri G, Calabi L, Aime S, Botta M. Inorg. Chem. 2003; 42:148. [PubMed: 12513089]
56. Kotek J, Rudovsky J, Hermann P, Lukes I. Inorg. Chem. 2006; 45:3097. [PubMed: 16562966]
57. Lebduskova P, Hermann P, Helm L, Toth E, Kotek J, Binnemans K, Rudovsky J, Lukes I, Merbach AE. Dalton Trans. 2007:493. [PubMed: 17213936]
58. Horrocks WD Jr. Arkle VK, Liotta FJ, Sudnick DR. J. Am. Chem. Soc. 1983; 105:3455.
59. Batsanov AS, Beeby A, Bruce JI, Howard JAK, Kenwright AM, Parker D. Chem. Commun. 1999:1011.
60. Banci L, Bertini I, Luchinat C. Inorg. Chim. Acta. 1985; 100:173.
61. Aime S, Botta M, Ermondi G. J. Magn. Reson. 1991; 92:572.
62. Costa J, Toth E, Helm L, Merbach AE. Inorg. Chem. 2005; 44:4747. [PubMed: 15962983]
63. Costa J, Balogh E, Turcryl V, Tripier R, Le Baccon M, Chuburu F, Handel H, Helm L, Toth E, Merbach AE. Chem. Eur. J. 2006; 12:6841. [PubMed: 16770815]
64. Koenig SH, Brown RD III. Prog. Nucl. Magn. Reson. Spectrosc. 1990; 22:487.
65. Ferreira MF, Mousavi B, Ferreira PM, Martins CIO, Helm L, Martins JA, Geraldes CFGC. Dalton Trans. 2012; 41:5472. [PubMed: 22467054]
66. Lipari G, Szabo A. J. Am. Chem. Soc. 1982; 104:4546.
67. Lipari G, Szabo A. J. Am. Chem. Soc. 1982; 104:4559.
68. Aime S, Botta M, Fedeli F, Gianolio E, Terreno E, Anelli P. Chem. Eur. J. 2001; 7:5261. [PubMed: 11822426]
69. Aime S, Botta M, Frullano L, Crich SG, Giovenzana GB, Pagliarin R, Palmisano G, Sisti M. Chem. Eur. J. 1999; 5:1253.
70. Gianolio E, Napolitano R, Fedeli F, Arena F, Aime S. Chem. Commun. 2009:6044.
71. Sudlow G, Birkett DJ, Wade DN. Mol. Pharmacol. 1975; 11:824. [PubMed: 1207674]
72. Sudlow G, Birkett DJ, Wade DN. Mol. Pharmacol. 1976; 12:1052. [PubMed: 1004490]
73. Caravan P, Cloutier NJ, Greenfield MT, McDermid SA, Dunham SU, Bulte JWM, Amedio JC Jr. Looby RJ, Supkowski RM, Horrocks WD Jr. McMurry TJ, Lauffer RB. J. Am. Chem. Soc. 2002; 124:3152. [PubMed: 11902904]
74. Yamasaki K, Maruyama T, Kragh-Hansen U, Otagiri M. Biochim. Biophys. Acta. 1996; 1295:147. [PubMed: 8695640]
75. Zech SG, Eldredge HB, Lowe MP, Caravan P. Inorg. Chem. 2007; 46:3576. [PubMed: 17425306]
76. Aime S, Gianolio E, Longo D, Pagliarin R, Lovazzano C, Sisti M. ChemBioChem. 2005; 6:818. [PubMed: 15791689]
77. Aime S, Botta M, Fasano M, Crich SG, Terreno E. J. Biol. Inorg. Chem. 1996; 1:312.
78. Powell DH, Ni Dhubhghaill OM, Pubanz D, Helm L, Lebedev YS, Schlaepfer W, Merbach AE. J. Am. Chem. Soc. 1996; 118:9333.
79. Toth E, Connac F, Helm L, Adzamli K, Merbach AE. J. Biol. Inorg. Chem. 1998; 3:606.
80. Payne KM, Aime S, Botta M, Valente E, Woods M. Chem. Commun. 2013:2320.
81. Hamilton JA, Chen L. J. Am. Chem. Soc. 1988; 110:5833.

82. Ponder JW, Case DA. Adv. Protein Chem. 2003; 66:27. [PubMed: 14631816]
83. Qiu D, Shenkin PS, Hollinger FP, Still WC. J. Phys. Chem. A. 1997; 101:3005.

SYNOPSIS: A divergence of expectation and reality

Theory often leads to an expectation that very fast water exchange is required to afford the highest relaxivity Gd^{3+} chelate. In practice, of two isomeric Gd^{3+} chelates, the one with the slowest water exchange affords the highest relaxivity.

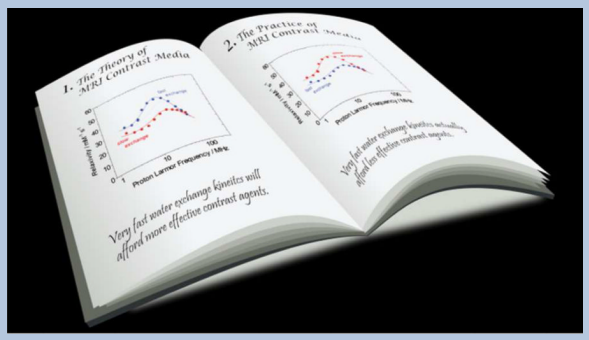

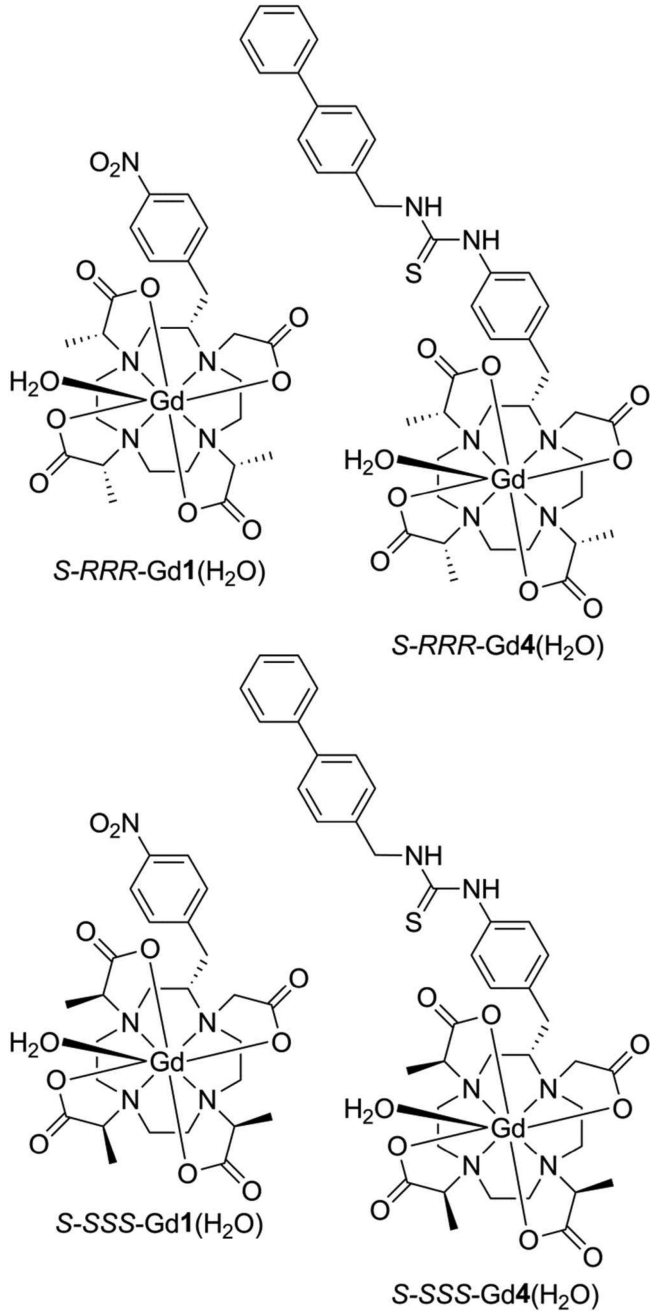

Chart 1.
The structures of conformationally rigid Ln^{3+} chelates.

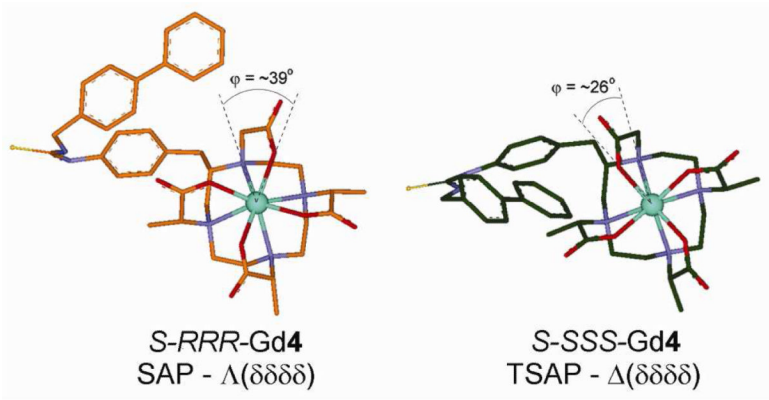

Figure 1.

The lowest energy conformations of *S-RRR*-Gd**4** (left, orange) and *S-SSS*-Gd**4** (right, green) obtained by Simulated Annealing Molecular Dynamics conformational analysis. These structures highlight the different coordination geometries of the two chelates characterized by different torsion angles (ϕ) and the position of the hydrophobic substituent – in each case located on the corner of the macrocyclic ring in an approximately similar position to that suggested by 2D NMR experiments.[47] Hydrogen atoms have been omitted for clarity.

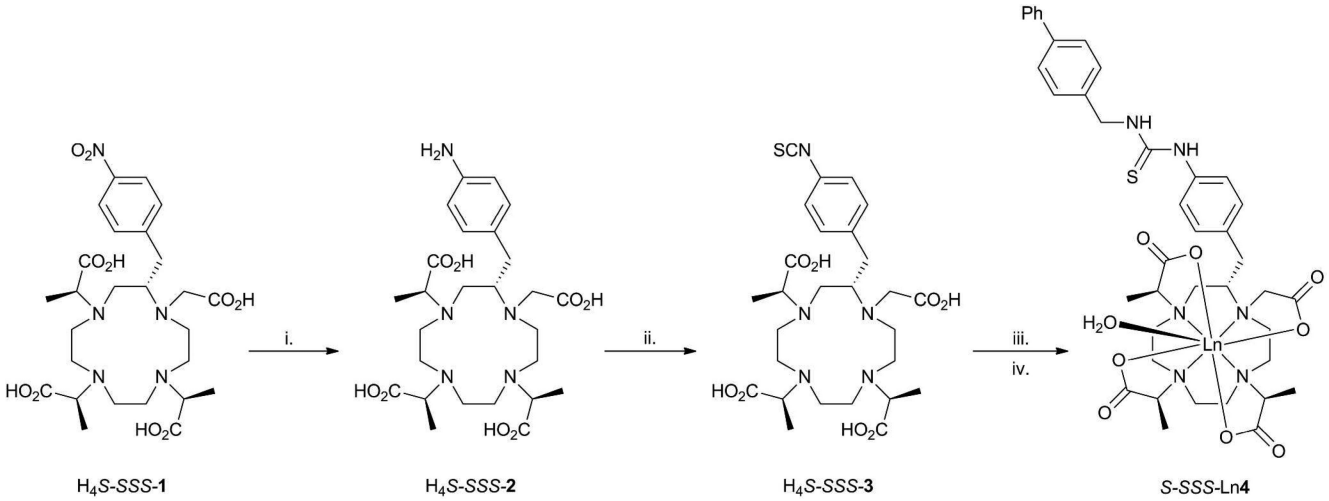

Scheme 1.

The synthesis of the lanthanide chelates of *S-SSS*-**4**, the chelates of *S-RRR*-**4** were synthesized according to the same synthetic scheme. *Reagents and conditions*: i. H_2 and 10% Pd on C; ii. $SCCl_2$ / $CHCl_3$ / H_2O pH 2; iii. 4-phenylbenzylamine / dioxane / H_2O pH 8; iv. $LnCl_3.6H_2O$, pH 6.

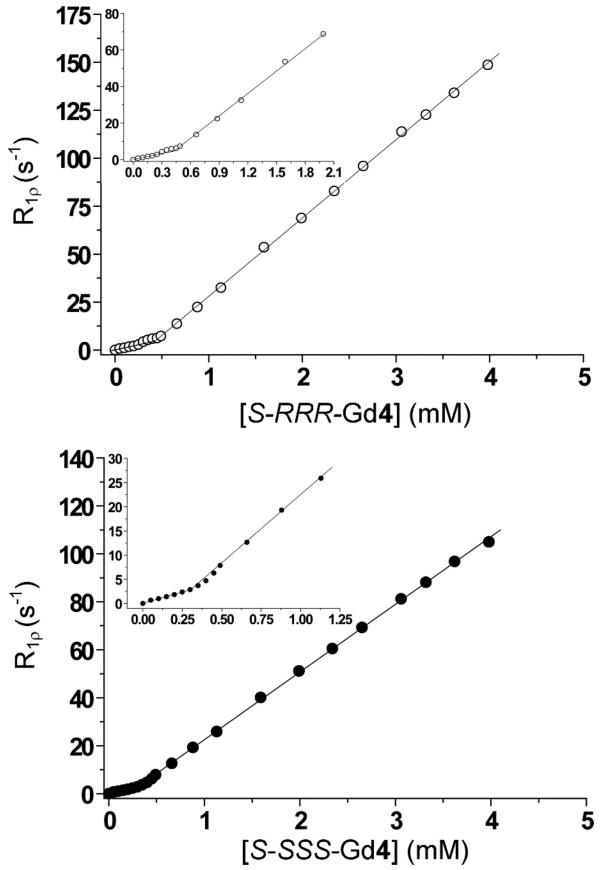

Figure 2.

Plots of the paramagnetic ^{1}H relaxation rate (R_{1p}) *versus* Gd^{3+} chelate concentration for *S*-*RRR*-Gd**4** (top) and *S*-*SSS*-Gd**4** (bottom) at 20 MHz and 25 °C, highlighting the change in relaxivity with changing chelate concentration.

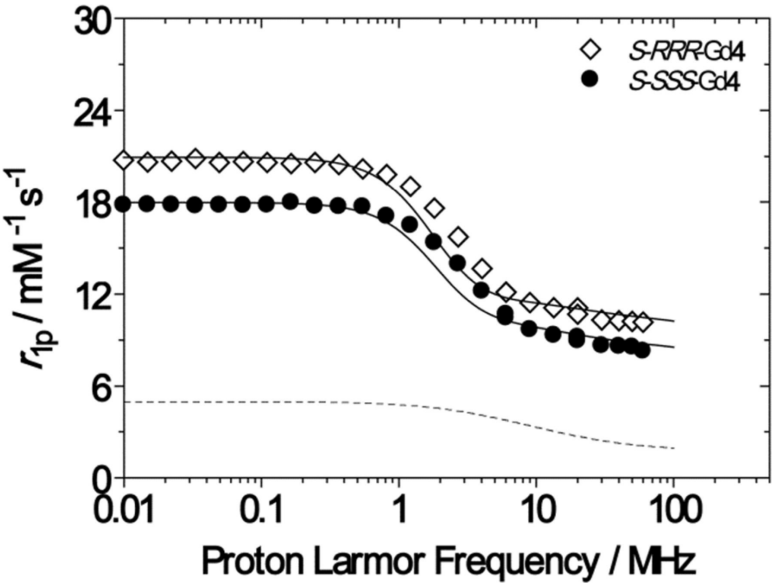

Figure 3.
The ^{1}H $1/T_1$ NMRD profiles of *S-RRR*-Gd**4** (SAP, open diamonds) and *S-SSS*-Gd**4** (TSAP, closed circles) recorded at 0.2 mM and 25 °C. Dashed lines represent the calculated outer-sphere contribution to relaxivities.

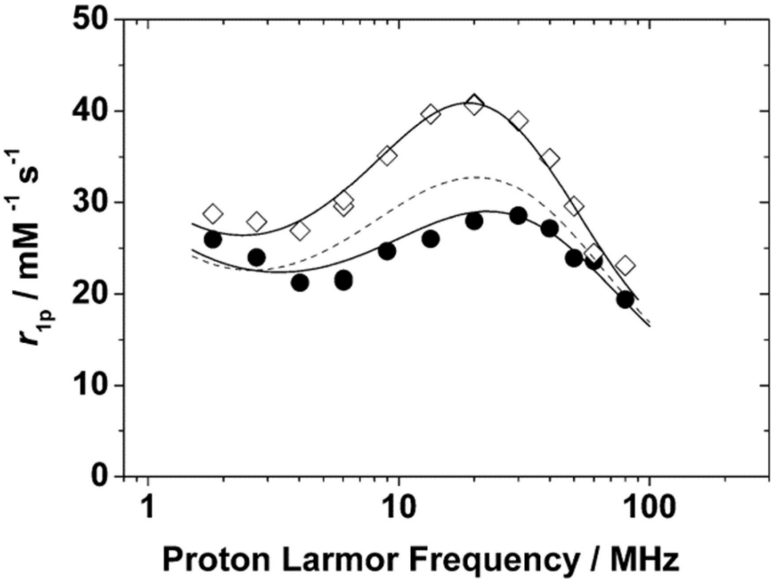

Figure 4.

The high field region of the ^{1}H $1/T_1$ NMRD profiles of *S-RRR*-Gd**4** (SAP, open diamonds) and *S-SSS*-Gd**4** (TSAP, closed circles) recorded at 3.98 mM and 25 °C. Solid lines represent fits to the data, the dashed line is a simulated profile taking the fitting parameters from the profile of *S-RRR*-Gd**4** but applying the water exchange parameters τ_M and r_{GdH} from the *S-SSS*-Gd**4** profile. Profiles including the low field region are provided in the supplementary information (S3, S5 & S7).

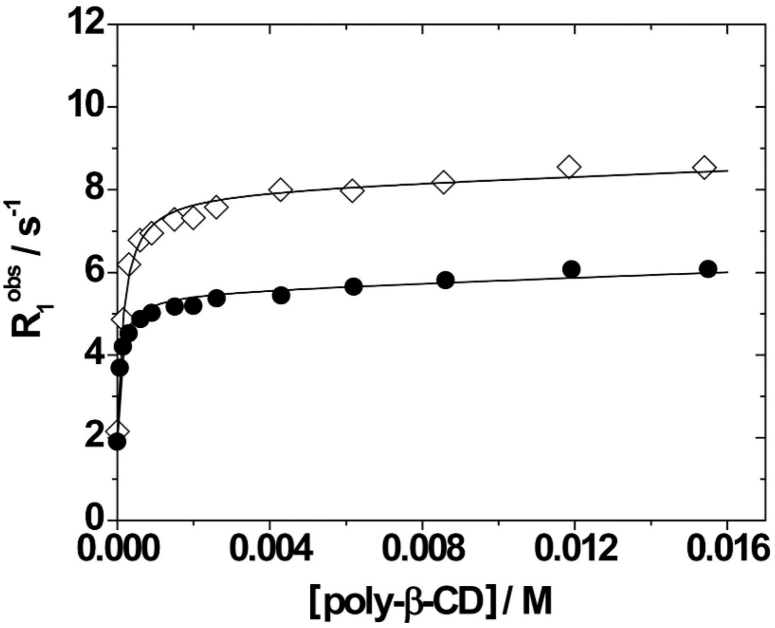

Figure 5.
The effect of poly-β-CD on the longitudinal relaxation rate (20 MHz, 25 °C) of dilute solutions (0.17 mM) of *S-RRR*-Gd**4** (SAP, open diamonds) and *S-SSS*-Gd**4** (TSAP, closed circles).

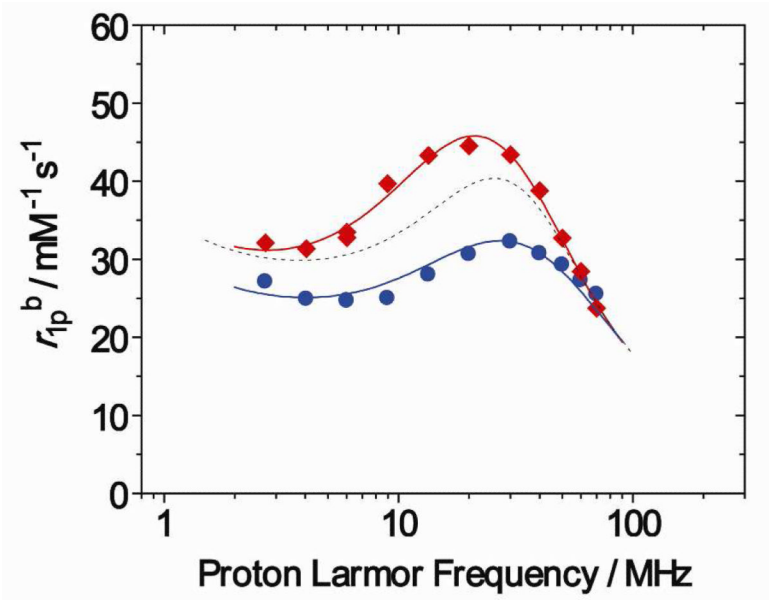

Figure 6.

The ^{1}H $1/T_1$ NMRD profiles of *S-RRR*-Gd**4** (red diamonds) and *S-SSS*-Gd**4** (blue circles) recorded at [Gd^{3+}] = 0.17 mM in the presence of 6 mM poly-β-CD at 25 °C.

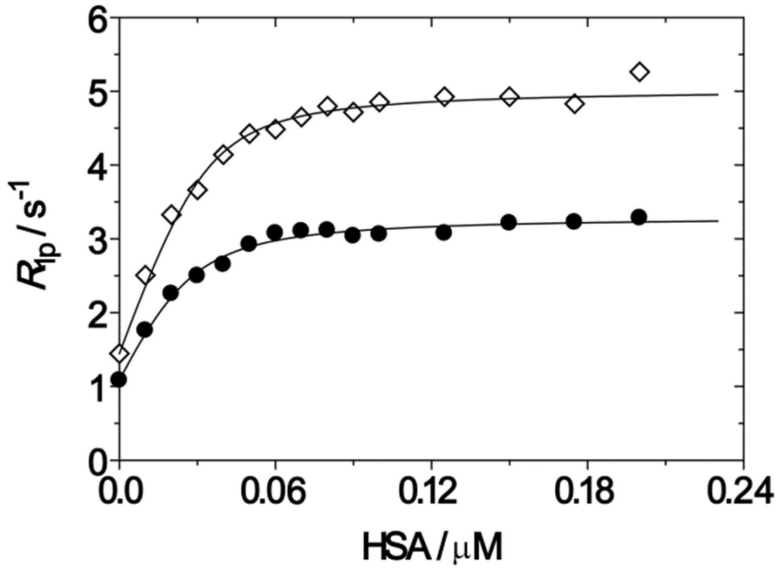

Figure 7.

Relaxometric titrations HSA of into 100 μM solutions of *S-RRR*-Gd**4** (SAP, open diamonds) and *S-SSS*-Gd**4** (TSAP, closed circles) at 20 MHz and 25 °C. A qualitative data fit is provided (Table 5) using a binding model with 3 equivalent binding sites.

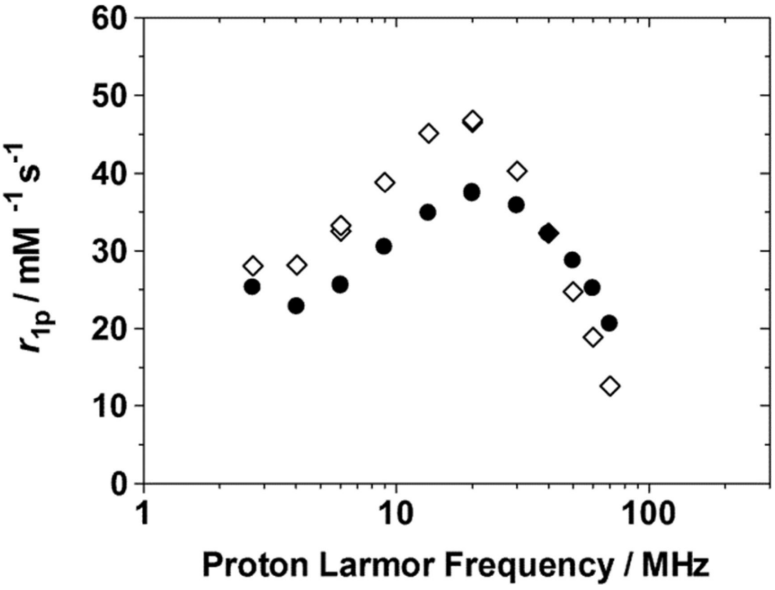

Figure 8.

The ^{1}H $1/T_1$ NMRD profiles of solutions of the two isomers of Gd**4** (0.15 mM) and HSA (1.8 mM): *S*-*RRR*-Gd**4** (open symbols); and *S*-*SSS*-Gd**4** (closed symbols) recorded at 25 °C.

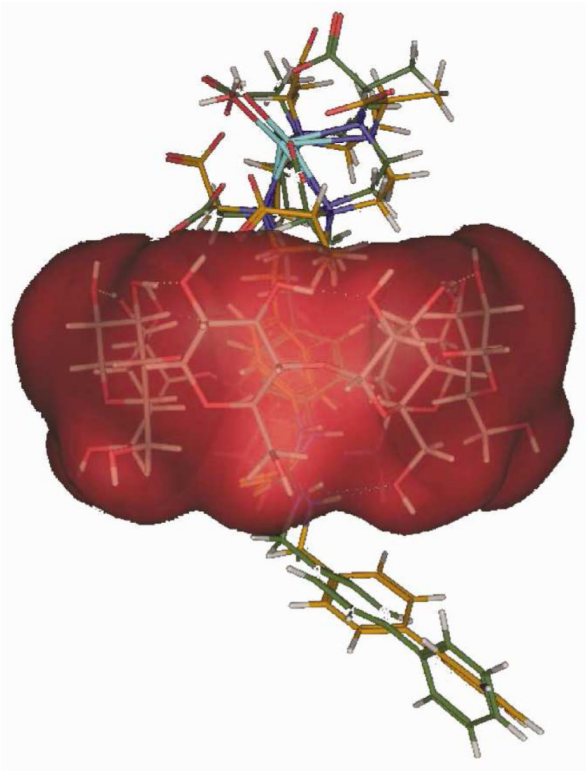

Figure 9.
Results of the calculated docking procedure applied to β-CD and *S-RRR*-Gd**4** (orange); and β-CD and *S-SSS*-Gd**4** (green). The β-CD surface is depicted with a red semi-transparent Gauss-Connolly surface. Both isomers place the *para*-phenyl group inside the hydrophobic cavity, with the thiourea moiety forming hydrogen bonding interactions with the primary hydroxyl groups of the narrow rim.

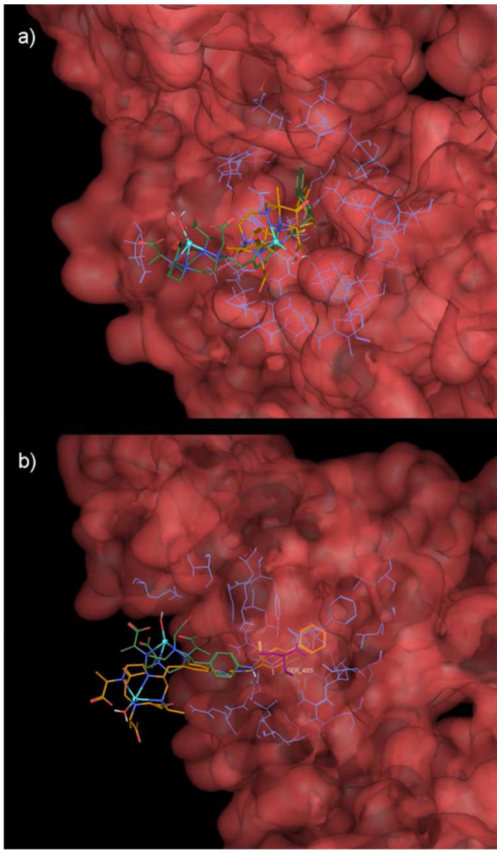

Figure 10.
Calculated docking of *S-RRR*-Gd**4** (orange); and β-CD and *S-SSS*-Gd**4** (green) to HSA: a) to drug binding site I; b) to drug binding site II. The hydrogen bonding interaction between S-SSS-Gd**4** with Ser489 (drug binding site II) is highlighted in purple. Hydrogen atoms have been omitted for clarity.

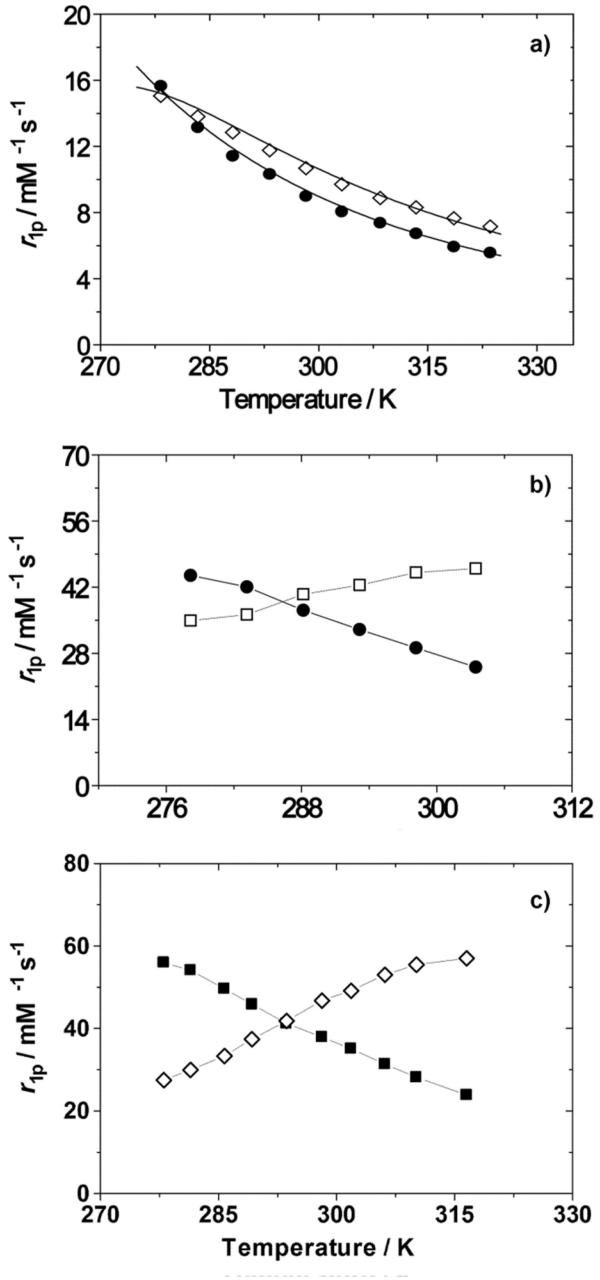

Figure 11.

Variation in the paramagnetic ^{1}H relaxivity of *S-RRR*-Gd**4** (open symbols) and *SSSS*-Gd**4** (closed circles) at 20 MHz: a) as discrete chelates in solution below the cmc; b) bound to poly β-CD; and c) bound to HSA at the same concentrations as in Figure 8. Solid lines are a) fits to the data and b) and c) a guide to the eyes only.

Table 1

Physicochemical properties of *S-RRR*-Gd**4** and *S-SSS*-Gd**4** obtained from the $1/T_1$ versus concentration plots in Figure 2.

Chelate	cmc[a] / mM	r_1 / $mM^{-1}s^{-1}$ below cmc	above cmc
S-RRR-Gd**4**	0.42 ± 0.02	10.7	40.8
S-SSS-Gd**4**	0.29 ± 0.02	9.0	28.2

[a]cmc = critical micelle concentration

Table 2

Best-fit parameters[a,b] of the NMRD profiles of *S-RRR*-Gd**4** and *S-SSS*-Gd**4** in Figures 3 and 4.

	[Gd^{3+}] = 0.20 mM		**[Gd^{3+}] = 3.98 mM**	
	***S-RRR*-Gd4**	***S-SSS*-Gd4**	***S-RRR*-Gd4**	***S-SSS*-Gd4**
$r_{Gd\text{-}H}$ / Å[b]	3.0	3.1	3.0	3.1
τ_M / ns[b]	70	8	70	8
Δ^2 / 10^{19} s^{-1}	0.62	0.61	2.4	2.6
τ_V / ps	42	45	29	20
τ_R / ps	229	220	-	-
τ_g / ns	-	-	3.84	3.38
τ_1 / ns	-	-	0.45	0.43
S^2	-	-	0.34	0.33

[a] Fitting used a = 3.8 Å, ^{298}D = 2.24×10^{-5} cm^2 s^{-1} and q = 1.

[b] parameter fixed during fitting.

Table 3

Fitting parameters for the binding of the two isomers of Gd**4** to poly-β-CD

	K_a / M^{-1}	r_1^{bound} / $mM^{-1}s^{-1}$ [a]
S-RRR-Gd**4**	0.51 ± 0.05 × 10^3	46 ± 0.7
S-SSS-Gd**4**	0.87 ± 0.07 × 10^3	30 ± 0.5

[a] Measured at 20 MHz and 25 °C.

Table 4

Best-fit parameters of the NMRD profiles (25 °C) of the inclusion complexes of the two isomers of Gd**4** with poly-β-CD.[a]

	***S*-*RRR*-Gd4**	***S*-*SSS*-Gd4**
$r_{Gd\text{-}H}$ / Å[b]	3.0	3.1
τ_M / ns[b]	70	8
Δ^2 / 10^{18} s^{-1}	2.8	3.7
τ_V / ps	18	12
τ_g / ns	4.2	3.6
τ_1 / ns	0.40	0.45
S^2	0.45	0.42

[a] Fitting used a = 3.8 Å, ^{298}D = 2.2×10^{-5} cm^2 s^{-1} and q = 1.

[b] parameter fixed during fitting.

Table 5

Binding parameters obtained from the qualitative fit of the relaxometric titration of HSA with *S-RRR*-Gd**4** and *S-SSS*-Gd**4** using a 3:1 binding model with equivalent binding sites.

	$K_{HSA\text{-}Gd4}$ ($\times 10^3$ M^{-1})[a]	r_1^{bound} ($mM^{-1}s^{-1}$)[a]
S-RRR-Gd**4**	71.3 ± 12.4	46.8 ± 0.9
S-SSS-Gd**4**	49.7 ± 7.9	37.6 ± 0.6

[a] apparent values (see text)

Table 6

The association constants of the two isomeric biphenyl conjugates Gd**4** in the two drug binding sites of HSA determined at 25 °C.

Fluorescent probe	Binding Site	$K_{HSA\text{-}Gd4}$ / M^{-1} *S-RRR*-Gd4	*S-SSS*-Gd4	MS-325[a]
Warfarin	I	n.d.	n.d.	n.d.
Dansyl sarcosine	II	$9.2 \pm 0.5 \times 10^{-3}$	$22.1 \pm 1.9 \times 10^{-3}$	11.8×10^{-3}

[a] taken from reference 73 and determined at 37 °C; n.d. indicates that no displacement of the fluorescent probe was detected.